Phase behaviour and structure of model colloid-polymer mixtures

1999 J. Phys.: Condens. Matter 11 10079

(http://iopscience.iop.org/0953-8984/11/50/304)

J. Phys.: Condens. Matter **11** (1999) 10079–10106. Printed in the UK PII: S0953-8984(99)06185-8

Phase behaviour and structure of model colloid–polymer mixtures

Marjolein Dijkstra†, Joseph M Brader and Robert Evans

H H Wills Physics Laboratory, University of Bristol, Royal Fort, Tyndall Avenue, Bristol BS8 1TL, UK

Received 21 July 1999

Abstract. We study the phase behaviour and structure of model colloid–polymer mixtures. By integrating out the degrees of freedom of the non-adsorbing ideal polymer coils, we derive a formal expression for the effective one-component Hamiltonian of the colloids. Using the two-body (Asakura–Oosawa pair potential) approximation to this effective Hamiltonian in computer simulations, we determine the phase behaviour for size ratios $q = \sigma_p/\sigma_c = 0.1$, 0.4, 0.6, and 0.8, where σ_c and σ_p denote the diameters of the colloids and the polymer coils, respectively. For large q, we find both a fluid–solid and a stable fluid–fluid transition. However, the latter becomes metastable with respect to a broad fluid–solid transition for $q \leqslant 0.4$. For $q = 0.1$ there is a metastable isostructural solid–solid transition which is likely to become stable for smaller values of q. We compare the phase diagrams obtained from simulation with those of perturbation theory using the same effective one-component Hamiltonian and with the results of the free-volume approach. Although both theories capture the main features of the topologies of the phase diagrams, neither provides an accurate description of the simulation results. Using simulation and the Percus–Yevick approximation we determine the radial distribution function $g(r)$ and the structure factor $S(k)$ of the effective one-component system along the fluid–solid and fluid–fluid phase boundaries. At state-points on the fluid–solid boundary corresponding to high colloid packing fractions (packing fractions equal to or larger than that at the triple point), the value of $S(k)$ at its first maximum is close to the value 2.85 given by the Hansen–Verlet freezing criterion. However, at lower colloid packing fractions freezing occurs when the maximum value is much lower than 2.85. Close to the critical point of the fluid–fluid transition we find Ornstein–Zernike behaviour and at very dilute colloid concentrations $S(k)$ exhibits pronounced small-angle scattering which reflects the growth of clusters of the colloids. We compare the phase behaviour of this model with that found in studies of additive binary hard-sphere mixtures.

(Some figures in this article appear in colour in the electronic version; see `www.iop.org`)

1. Introduction

In 1954, Asakura and Oosawa showed that when two large (colloidal) bodies are immersed in a solvent consisting of smaller macromolecules, an effective attractive interaction is induced between the two bodies due to an unbalanced osmotic pressure arising from depletion of the macromolecules in the region between the bodies [1]. The range of this effective interaction is equal to the size of the macromolecules and the strength of the attraction is proportional to the osmotic pressure of these [1]. Independently, and more than twenty years later, Vrij showed that attractive interactions are induced between the colloids in colloid–polymer mixtures due to the presence of the non-adsorbing polymers [2]. Moreover, he demonstrated the existence of

† Permanent address: Debye Institute and Institute of Theoretical Physics, University of Utrecht, Princetonplein 5, 3584 CC Utrecht, The Netherlands.

0953-8984/99/5010079+28$30.00

a spinodal instability in what is now termed the Asakura–Oosawa model. In this simple model for the colloid–polymer mixture, the colloids are modelled as hard spheres with diameter σ_c, whereas the polymer coils are treated as interpenetrating, non-interacting particles as regards their mutual interactions. However, the polymers are excluded by a centre-of-mass distance of $(\sigma_c + \sigma_p)/2$ from the colloids where σ_p, the diameter of the polymer coil, is given by $\sigma_p = 2R_g$ with R_g the radius of gyration of the polymer. In the same paper, Vrij also presented experimental evidence for fluid–fluid separation in a mixture of silica particles and polystyrene [2]. A few years later, Gast *et al* [3] employed an effective-pairwise-potential model based on the Asakura–Oosawa depletion potential to calculate the phase equilibria for colloid–polymer mixtures. Using a standard liquid-state perturbation theory with the hard-sphere system as a reference, they found that the addition of polymer broadens the fluid–solid coexistence region enormously when the size of the polymer coils is small compared to that of the colloids. In addition, for sufficiently large size ratios $q = \sigma_p/\sigma_c$ a stable fluid–fluid and a three-phase coexistence of a colloidal gas, liquid, and solid were found. Phase diagrams with similar topologies as functions of q were found by Lekkerkerker *et al* using the so-called free-volume approach [4]. The key quantity in this approach is the statistically averaged volume that is available for the polymers at a given polymer fugacity. Using a low-density expansion for the polymers and employing scaled-particle expressions for the volume that is available in the hard-sphere system, the free energy is then obtained directly, since the polymers are assumed ideal. Experimental studies of colloid–polymer mixtures corroborated the existence of a stable fluid–fluid (gas–liquid) phase separation and also showed that this has a sensitive dependence on the size ratio [5,6]. While it is now well accepted that the topology of the phase diagram of colloid–polymer mixtures depends critically on the size of the polymer coils, or equivalently on the range and strength of the effective attractive interactions induced by the presence of the polymers, a full understanding of the systematics is still lacking.

There is less information on the *structure* of these mixtures. As most theoretical approaches are based on perturbation theories, taking the hard-sphere system as a reference, little detailed structural information has been obtained. However, more experimental data are becoming available on the structure of these mixtures. Static colloid–colloid structure factors $S(k)$ were measured recently in the colloidal liquid phase at triple coexistence, for different size ratios, using a novel application of two-colour dynamic light scattering [7]. There are also recent neutron scattering determinations of $S(k)$ for a series of size ratios and polymer concentrations [8]. The new experimental results [7] motivated Louis *et al* [9] to calculate the three partial structure factors for the Asakura–Oosawa model using the Percus–Yevick approximation. Although the authors claim that their theoretical results compare reasonably well with those of the experiments, direct comparisons between the two sets of data are difficult to make since the phase behaviour was not determined within the integral equation theory, i.e. one does not know whether the theoretical results for $S(k)$ correspond to state-points that are close to the solid–fluid phase boundaries or, indeed, to three-phase coexistence†.

In this paper, we attempt a systematic investigation of the phase equilibria and the structure of the Asakura–Oosawa model of colloid–polymer mixtures using computer simulation. Our aims are to assess the reliability of the existing theories for the phase behaviour of this model system and to examine the predictions for the colloid–colloid pairwise correlation functions.

† Note that the state-point ($\eta_c = 0.404$, $\eta_p^r = 0.6$) for size ratio $q = 0.37$ in figure 4 of reference [9] for the Asakura–Oosawa pair potential is well inside the fluid–solid coexistence region obtained in our simulation (see figure 1(b), later). If we compare the state-point ($\eta_c = 0.404$, $\eta_p = 0.15$) for the binary Asakura–Oosawa model considered in the same figure with the phase diagram calculated from the free-volume approach [4], we find that this also lies well inside the fluid–solid region.

It is well known that direct simulation of the Asakura–Oosawa model, which is a highly asymmetric non-additive binary mixture, is prohibited by slow equilibration, as huge numbers of polymers are needed per colloid particle at the state-points of interest. Previous simulation studies [10] represented the polymers by ideal particles on a lattice or by lattice chains. Another way to circumvent this problem is to take advantage of the large size asymmetry by mapping the binary mixture onto an effective one-component system. Recently, it was shown that an effective one-component Hamiltonian for the large spheres can be derived for a binary hard-sphere mixture by formally integrating out the degrees of freedom of the smaller spheres [11]. This effective Hamiltonian consists of zero-body, one-body, two-body, and higher-body terms. The phase behaviour and pair correlation functions of the large spheres are then determined by Monte Carlo simulations of an approximation to the effective Hamiltonian [11]. A similar approach is applied here to the Asakura–Oosawa model. The zero- and one-body terms are much simpler in this case and the two-body (pairwise-additive) term is precisely that given by the Asakura–Oosawa pair potential. Moreover, for size ratios $q < 0.154$, three-body and higher-body terms are identically zero, so the mapping to the two-body approximation to this effective Hamiltonian is exact in this regime. We perform Monte Carlo simulations for the effective Hamiltonian truncated at the pairwise term, i.e. using the Asakura–Oosawa pair potential, and we determine the phase behaviour and structure of the effective one-component system for size ratios $q = 0.1$, 0.4, 0.6, and 0.8.

The paper is organized as follows. In section 2, we describe the model and derive an explicit expression for the effective one-component Hamiltonian by integrating out the degrees of freedom of the polymer coils. In section 3, we present results of computer simulations based on the approximate effective Hamiltonian. Phase diagrams and the pairwise correlation functions are shown for each size ratio. In section 4 the phase diagrams are compared with those from the perturbation theory treatment of this effective Hamiltonian and with those from the free-volume approach. In section 5, we compare the phase diagrams calculated in perturbation theory for the Asakura–Oosawa pair potential model, i.e. for the binary non-additive hard-sphere mixture, with the corresponding ones for the additive binary hard-sphere mixture. Although these share some common features there are significant differences in the variation of the phase equilibria with size ratio. We conclude, in section 6, with a summary and discussion of our results.

2. Model

We consider a suspension of sterically stabilized colloidal particles immersed together with non-adsorbing polymers in an organic solvent. As the differences in length scales and time scales between the solvent molecules and the colloids and polymers are huge, we can assume the solvent to be an inert continuum, thereby ignoring the degrees of freedom of the individual solvent molecules. Within this framework, effective potentials between the colloidal particles and the polymers can be envisaged, and these are often assumed to be pairwise additive. The interaction between two sterically stabilized colloidal particles in an organic solvent is close to that between hard spheres, whereas dilute solutions of polymers in a theta-solvent can be represented by non-interacting or ideal polymers. A simple idealized model for such a colloid–polymer mixture is the so-called Asakura–Oosawa model. This is an extreme non-additive binary hard-sphere model in which the colloids are treated as hard spheres with diameter σ_c and the interpenetrable, non-interacting polymer coils are treated as point particles but which are excluded from the colloids to a centre-of-mass distance of $(\sigma_c + \sigma_p)/2$. The diameter of the polymer coil is $\sigma_p = 2R_g$ with R_g the radius of gyration of the polymer. The pairwise

potentials in this simple model are given by

$$\begin{aligned}
\phi_{cc}(\boldsymbol{R}_{ij}) &= \begin{cases} \infty & \text{for } |\boldsymbol{R}_{ij}| < \sigma_c \\ 0 & \text{otherwise} \end{cases} \\
\phi_{cp}(\boldsymbol{R}_i - \boldsymbol{r}_j) &= \begin{cases} \infty & \text{for } |\boldsymbol{R}_i - \boldsymbol{r}_j| < \frac{1}{2}(\sigma_c + \sigma_p) \\ 0 & \text{otherwise} \end{cases} \\
\phi_{pp}(\boldsymbol{r}_{ij}) &= 0.
\end{aligned} \tag{1}$$

Here $\boldsymbol{R}_i$ and $\boldsymbol{r}_j$ are the positions of the centres of the colloids and the polymer coils, respectively, while $\boldsymbol{R}_{ij} = \boldsymbol{R}_i - \boldsymbol{R}_j$ and $\boldsymbol{r}_{ij} = \boldsymbol{r}_i - \boldsymbol{r}_j$. Most theoretical studies of colloid–polymer mixtures are based on this Asakura–Oosawa model. However, even within the context of the model it has been necessary to make approximations or assumptions in order to arrive at quantitative predictions for the phase behaviour, and the calculated phase behaviour and structure appear to be very sensitive to the precise details of the assumptions. In this paper, we take advantage of the large size asymmetry, and integrate out the degrees of freedom of the (small) polymer coils to obtain an effective Hamiltonian for the (large) colloids. Below, we describe briefly how we map the binary mixture of colloids and polymers with interaction Hamiltonian H onto an effective one-component system with Hamiltonian H^{eff}. Our derivation follows that in reference [11].

Thus, we consider N_c colloids and N_p ideal polymer coils with size ratio q in a macroscopic volume V at temperature T. The total Hamiltonian consists of (trivial) kinetic energy contributions and a sum of interaction terms:

$$H = H_{cc} + H_{cp} + H_{pp}$$

where

$$\begin{aligned}
H_{cc} &= \sum_{i<j}^{N_c} \phi_{cc}(\boldsymbol{R}_{ij}) \\
H_{cp} &= \sum_{i=1}^{N_c} \sum_{j=1}^{N_p} \phi_{cp}(\boldsymbol{R}_i - \boldsymbol{r}_j) \\
H_{pp} &= \sum_{i<j}^{N_p} \phi_{pp}(\boldsymbol{r}_{ij}) = 0.
\end{aligned} \tag{2}$$

It is convenient to consider the system in the (N_c, V, z_p, T) ensemble, in which the fugacity

$$z_p = \Lambda_p^{-3} \exp(\beta \mu_p)$$

of the polymer coils is fixed. Here μ_p denotes the chemical potential of the reservoir of polymer coils and $\beta = 1/k_B T$. The thermodynamic potential $F(N_c, V, z_p)$ of this system can be written as

$$\begin{aligned}
\exp[-\beta F] &= \sum_{N_p=0}^{\infty} \frac{z_p^{N_p}}{N_c! \Lambda_c^{3N_c} N_p!} \int_V \mathrm{d}\boldsymbol{R}^{N_c} \int_V \mathrm{d}\boldsymbol{r}^{N_p} \ \exp[-\beta(H_{cc} + H_{cp})] \\
&= \frac{1}{N_c! \Lambda_c^{3N_c}} \int_V \mathrm{d}\boldsymbol{R}^{N_c} \ \exp[-\beta H^{\text{eff}}]
\end{aligned} \tag{3}$$

where $H^{\text{eff}} = H_{cc} + \Omega$ is the effective Hamiltonian of the colloids, and Λ_ν is the thermal wavelength of species ν. Here Ω is the grand potential of the fluid of ideal polymer coils in the

external field of a fixed configuration of N_c colloids with coordinates $\{\boldsymbol{R}_i\}$; $i = 1, 2, \ldots, N_c$:

$$\begin{aligned}\exp[-\beta\Omega] &= \sum_{N_p=0}^{\infty} \frac{z_p^{N_p}}{N_p!} \int_V \mathrm{d}\boldsymbol{r}^{N_p} \ \exp[-\beta H_{cp}] \\ &= \sum_{N_p=0}^{\infty} \frac{z_p^{N_p}}{N_p!} \left(\int_V \mathrm{d}\boldsymbol{r}_j \ \exp\left[-\sum_{i=1}^{N_c} \beta\phi_{cp}(\boldsymbol{R}_i - \boldsymbol{r}_j) \right] \right)^{N_p} \\ &= \exp\left[z_p \int_V \mathrm{d}\boldsymbol{r}_j \ \exp\left[-\sum_{i=1}^{N_c} \beta\phi_{cp}(\boldsymbol{R}_i - \boldsymbol{r}_j) \right] \right]. \end{aligned} \tag{4}$$

Once Ω, and thus H^{eff}, are known for all values of z_p, the thermodynamics and the phase behaviour of the mixture can be determined. To this end, we expand Ω in terms of the Mayer function

$$f_{ij} \equiv f(\boldsymbol{R}_i, \boldsymbol{r}_j) = \exp[-\beta\phi_{cp}(\boldsymbol{R}_i - \boldsymbol{r}_j)] - 1$$

and find

$$\begin{aligned} -\beta\Omega &= z_p \int_V \mathrm{d}\boldsymbol{r}_j \ \prod_{i=1}^{N_c} (1 + f_{ij}) \\ &= z_p \int_V \mathrm{d}\boldsymbol{r}_j + \sum_{i=1}^{N_c} z_p \int_V \mathrm{d}\boldsymbol{r}_j \ f_{ij} + \sum \sum_{i<k}^{N_c} z_p \int_V \mathrm{d}\boldsymbol{r}_j \ f_{ij} f_{kj} \\ &\quad + \sum \sum_{i<k<l}^{N_c} \sum z_p \int_V \mathrm{d}\boldsymbol{r}_j \ f_{ij} f_{kj} f_{lj} + \cdots . \end{aligned} \tag{5}$$

Using standard diagrammatic techniques [11, 12], we can rewrite $-\beta\Omega$ in terms of diagrams:

$-\beta\Omega =$ 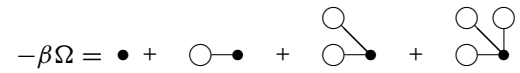 (6)

where (i) each black circle represents a factor z_p and an integral of $\boldsymbol{r}_j$ over the volume V, and (ii) each open big circle connected with a black circle represents an f-bond and a summation over all different colloids at positions $\boldsymbol{R}_i$ for $i = 1, \ldots, N_c$. The grand potential Ω can then be classified according to the number $n = 0, 1, 2, \ldots, N_c$ of colloids that interact simultaneously with the 'sea' of ideal polymer, so

$$\beta\Omega = \sum_{n=0}^{N_c} \beta\Omega_n .$$

We give explicit expressions for $\beta\Omega_n$ for $n = 0$, 1, and 2. Since the polymers are assumed to be non-interacting, the expansion (6) is, of course, much simpler than the corresponding result for binary hard-sphere mixtures [11] where extra classes of diagrams, containing small–small Mayer bonds, appear.

The first diagram, $-\beta\Omega_0$, is equal to $z_p V$ and is the grand potential of a pure system of ideal polymer at fugacity z_p in a volume V. For an ideal polymer, z_p can be replaced by $\beta p^r(z_p)$ or by $\rho_p^r(z_p)$, where $p^r(z_p)$ is the pressure and $\rho_p^r(z_p)$ is the density of the ideal polymer in the corresponding reservoir. It follows directly from equation (5) that the second diagram, $-\beta\Omega_1$, can be interpreted as $-z_p N_c$ times the volume that is excluded for a polymer coil by a single colloid. Thus, we find

$$-\beta\Omega_1 = -z_p \eta_c (1 + q)^3 V \tag{7}$$

where $\eta_c = (\pi/6)\sigma_c^3 N_c/V$ is the colloid packing fraction. Ω_2 can be written as a sum of pair potentials:

$$\Omega_2 = \sum_{i<j}^{N_c} \phi_{\rm AO}(R_{ij})$$

where we can show that $\beta z_p^{-1}\phi_{\rm AO}(R_{ij})$ is the difference in free volume of the polymers when *two* colloids are separated by a finite distance $R_{ij} \equiv |\boldsymbol{R}_i - \boldsymbol{R}_j|$ and when they are separated by infinite distance. The exact expression for the potential was derived by Asakura and Oosawa [1]:

$$\beta\phi_{\rm AO}(R_{ij}) = \begin{cases} -\dfrac{\pi\sigma_p^3 z_p}{6}\dfrac{(1+q)^3}{q^3} & \\ \quad \times \left[1 - \dfrac{3R_{ij}}{2(1+q)\sigma_c} + \dfrac{R_{ij}^3}{2(1+q)^3\sigma_c^3}\right] & \text{for } \sigma_c < R_{ij} < \sigma_c + \sigma_p \\ 0 & \text{for } R_{ij} > \sigma_c + \sigma_p. \end{cases} \tag{8}$$

This Asakura–Oosawa pair potential describes an attractive potential well close to the surface of the colloid, whose depth increases linearly with increasing z_p. The range of the potential is given by σ_p.

The higher-order Ω_n correspond to n-body potentials. For size ratios $q < 0.154$, three or more non-overlapping colloids cannot simultaneously overlap with a small one [3], and diagrams consisting of three or more open big circles are identically zero in equation (6). For these small size ratios, the mapping of the two-component Asakura–Oosawa model onto the effective one-component Hamiltonian based on pairwise additive Asakura–Oosawa potentials is exact. More precisely, the effective one-component Hamiltonian

$$H^{\rm eff} = H_0 + \sum_{i<j}^{N_c} \phi_{\rm eff}(R_{ij}) \tag{9}$$

with effective pair potential

$$\phi_{\rm eff}(R_{ij}) = \phi_{cc}(R_{ij}) + \phi_{\rm AO}(R_{ij})$$

and

$$\beta H_0 \equiv \beta(\Omega_0 + \Omega_1) = -z_p(1 - \eta_c(1+q)^3)V$$

should generate thermodynamic properties and (equilibrium) correlation functions which are identical to those from the original Asakura–Oosawa model of the binary fluid. Note that since H_0 is independent of the coordinates $\{\boldsymbol{R}_i\}$ of the colloids, this term does not influence the colloid–colloid correlation functions; these are determined for a given polymer fugacity, size ratio, and colloid density by the pair potential $\phi_{\rm eff}$. Moreover, since H_0/V is linear in the colloid density, this term does not affect the phase equilibria, although it does contribute to the pressure of the colloid–polymer mixture. This scenario is equivalent to that for the additive hard-sphere mixture [11]. However, it is important to recognize that in the additive case the corresponding pairwise effective Hamiltonian is not exact, as higher-body potentials, arising from non-vanishing small–small interactions, persist even for $q \leqslant 0.154$.

When the size ratio $q \geqslant 0.154$, three-body and certain higher-body terms will be non-zero. More precisely, we expect an increasing number of higher-body terms to become non-zero when q increases. This can be made plausible by geometric arguments, since the number of non-overlapping colloidal spheres that can simultaneously overlap with a polymer coil increases when q increases. In what follows we shall set $\Omega_n = 0$ for $n \geqslant 3$ and employ the

effective Hamiltonian (9) for all values of q. This is then equivalent to the approach adopted in the pioneering study by Gast *et al* [3]. Their effective Hamiltonian is simply postulated to be the second (pairwise) contribution in (9). As they did not perform a systematic integrating out of the polymer degrees of freedom they do not obtain H_0 or the higher-n (>2)-body potentials. As q increases higher-body terms should play an increasingly important role.

3. Results of simulations using the effective Hamiltonian

3.1. Phase diagram

In order to determine the phase diagram of the effective one-component system, we first calculate the thermodynamic potential F, defined in equation (3) with $H_{\rm eff}$ given by (9), as a function of N_c, V, and z_p. For convenience we usually replace the dependence on z_p by that on the reservoir packing fraction η_p^r. As the free energy cannot be measured directly in a Monte Carlo simulation, we use thermodynamic integration to relate the free energy of the effective system to that of a reference hard-sphere system at the same colloid packing fraction η_c. To this end we introduce the auxiliary effective Hamiltonian

$$H_\lambda^{\rm eff} = \sum_{i<j}^{N_c} (\phi_{cc}(R_{ij}) + \lambda \phi_{\rm AO}(R_{ij})) \tag{10}$$

where $0 \leqslant \lambda \leqslant 1$ is a dimensionless coupling parameter: at $\lambda = 0$ the auxiliary Hamiltonian is that of the pure system of N_c hard spheres, while at $\lambda = 1$ it is the effective Hamiltonian of interest (for fixed z_p and V). It is a standard result [13–15] that

$$F(N_c, V, z_p) = F(N_c, V, z_p = 0) + \int_0^1 {\rm d}\lambda \left\langle \sum_{i<j}^{N_c} \phi_{\rm AO}(R_{ij}) \right\rangle_{N_c, V, z_p, \lambda} \tag{11}$$

where $F(N_c, V, z_p = 0)$ is the free energy of the pure reference system of hard spheres ($\lambda = 0$), for which we use the Carnahan–Starling expression [16] for the fluid, and the analytic form for the equation of state proposed by Hall [17] for the solid phase. In the latter case an integration constant is determined such that the simulation results for fluid–solid coexistence of the pure hard-sphere system are recovered [18]. The angular brackets $\langle \cdots \rangle_{N_c, V, z_p, \lambda}$ denote a canonical average over the system of N_c colloids interacting via the auxiliary Hamiltonian $H_\lambda^{\rm eff}$. The integrand in equation (11) can, for a fixed λ, be measured in a standard MC calculation; for the numerical λ-integration we use a ten-point Gauss–Legendre quadrature [19].

In order to map out the phase diagram the free-energy density $f = F/V$ must be determined from λ-integrations for many state-points (η_c, z_p). We chose therefore to simulate relatively small systems, with $N_c = 108$. We employ common-tangent constructions at fixed z_p to obtain the coexisting phases, i.e. we fitted polynomials to f and computed the pressure and chemical potential at each η_c. The densities of the coexisting phases can then be determined by equating the pressures and chemical potentials in both phases. For more details we refer the reader to reference [11].

The above procedure has been carried out to determine the phase diagrams for size ratios $q = 0.1$, 0.4, 0.6, and 0.8. In figure 1, we show the resulting phase diagrams in the (η_c, η_p^r) plane. This representation, which is the natural one given our approach, implies that the tie lines connecting coexisting state-points are horizontal. At $\eta_p^r = 0$ our procedure ensures that we recover the known freezing transition of the pure hard-sphere system for all q. We have not calculated the actual polymer packing fraction η_p in each of the coexisting phases of the binary mixture so we have not determined the tie lines in the (η_c, η_p) plane. η_p can be obtained from simulations of the effective Hamiltonian and we shall discuss this topic in a future publication.

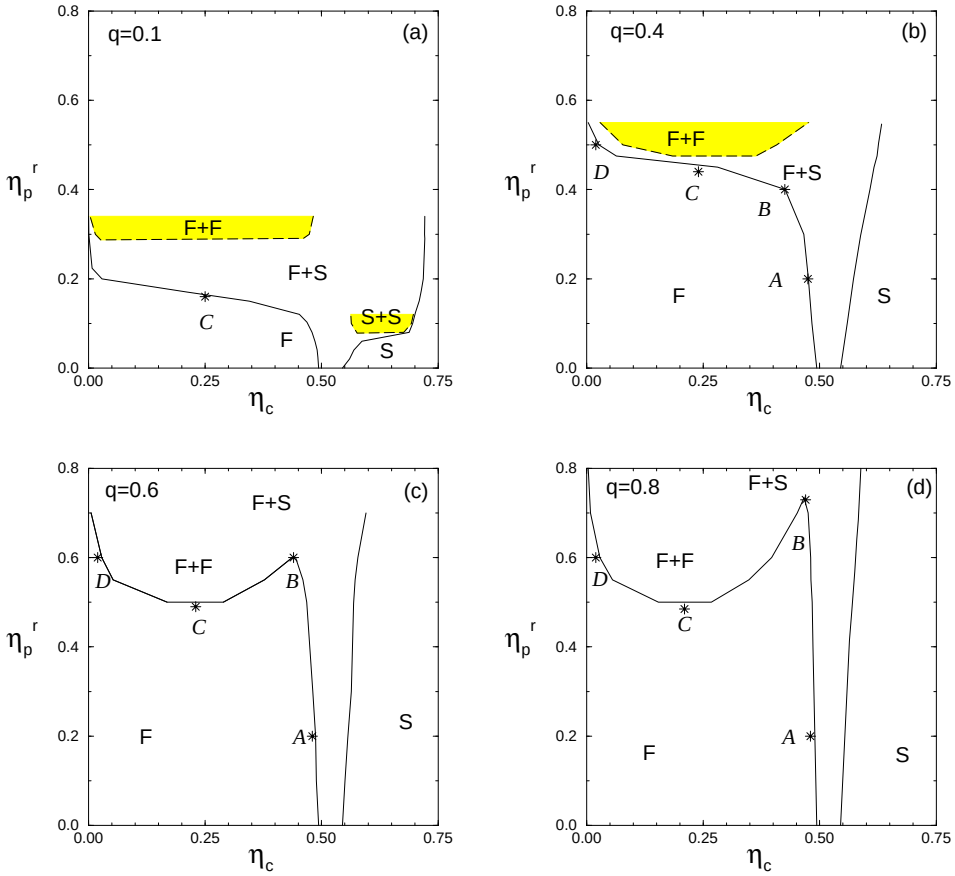

Figure 1. Phase diagrams of model colloid–polymer mixtures with size ratios (a) $q = \sigma_p/\sigma_c = 0.1$, (b) $q = 0.4$, (c) $q = 0.6$, and (d) $q = 0.8$ as functions of the colloid packing fraction η_c and the ideal polymer coil reservoir packing fraction η_p^r as obtained from simulations of the effective one-component Hamiltonian. F and S denote the stable fluid and solid (fcc) phase. F + S, F + F, and S + S denote, respectively, the stable fluid–solid, the (meta)stable fluid–fluid, and the metastable solid–solid coexistence region. The asterisks denote state-points at which pairwise correlation functions were calculated.

For $q \leqslant 0.4$, an enormous widening of the fluid–solid transition is observed when η_p^r increases sufficiently. This implies that the coexisting fluid and solid phase become progressively more dilute and dense, respectively, upon increasing η_p^r. This widening is consistent with earlier findings by Gast *et al* [3] in perturbation theory studies of the same pair potential model (see section 4.1). It has also been observed in experiments on colloid–polymer mixtures [5, 6] and in simulations of hard spheres and lattice polymers [10]. The shape of the coexistence curves implies that for small values of q the fluid phase only persists to very low values of η_c when η_p^r is sufficiently high. The calculations also reveal the existence of a fluid–fluid transition. However, for $q = 0.1$ and 0.4 we find this fluid–fluid coexistence is metastable with respect to the broad fluid–solid transition. For $q \geqslant 0.6$ the fluid–fluid coexistence becomes stable. Assuming a linear dependence on q of the difference between the polymer reservoir packing fraction at the triple point and at the critical point, we can estimate that the liquid phase becomes metastable for size ratios $q \leqslant 0.45$. This value of the size ratio

is equal to the corresponding crossover value estimated from direct simulations of a lattice version of the Asakura–Oosawa model, in which the polymer spheres are restricted to a cubic lattice [10], but which make no other approximation. Thus the crossover value, where the liquid state becomes 'marginal', appears not to be sensitive to the neglect of three-body and higher-body terms. However, if we compare our phase diagrams with those of reference [10], we find that for a given q our critical point and triple point are both located at lower polymer reservoir packing fractions and that the difference between the polymer reservoir packing fractions at the critical point and at the triple point is severely underestimated.

For $q = 0.1$, the phase diagram exhibits an isostructural solid–solid transition, i.e. coexistence between two face-centred-cubic (fcc) colloidal crystal phases. This solid–solid coexistence region is found to be metastable with respect to the solid–fluid transition, although the critical point of the solid–solid binodal is very close to the stable fluid–solid phase boundary. Note that for small reservoir packing fractions η_p^r, the effective pairwise (depletion) potential of additive binary hard-sphere mixtures reduces to the Asakura–Oosawa pair potential. Thus one expects very similar phase equilibria for the two types of mixture at small values of the reservoir packing fraction. Since the phase boundaries of the additive hard-sphere mixture shift to small reservoir packing fractions for small values of q [11], the phase boundaries for very asymmetric additive hard-sphere mixtures should resemble those of very asymmetric non-additive colloid–polymer mixtures. Indeed, the location of the solid–solid transition in our model colloid–polymer mixture for $q = 0.1$ is very close to its location in the phase diagram of the additive hard-sphere mixture at the same size ratio [11]. For more extreme size ratios the phase boundaries of the present effective one-component Hamiltonian should lie even closer to those obtained from the effective Hamiltonian description of the additive binary hard-sphere mixture. Thus for $q = 0.05$ and 0.033, the cases considered in reference [11], the phase boundaries of the present model resemble closely those computed in [11]. As the latter results show that the solid–solid coexistence becomes stable for $q \leqslant 0.05$, it follows that solid–solid coexistence should also be stable in the same range of q for the present effective Hamiltonian. This conclusion takes on more significance when we recall that for $q < 0.154$ the mapping to the effective one-component Hamiltonian (9) is exact. We may infer that the full Asakura–Oosawa model of the colloid–polymer mixture will exhibit a stable solid–solid transition for $q \leqslant 0.05$.

3.2. Colloid–colloid structure

In this subsection we turn our attention to the structure of the model colloid–polymer mixtures. Given that we determined the phase diagrams in subsection 3.1, we can now calculate the colloid–colloid radial distribution function $g(r)$ and the structure factor $S(k)$ in the fluid phase but close to the phase boundaries. We performed simulations with $N_c = 1000$ colloids, interacting with the same effective pair potential that we used to calculate the phase diagrams. The structure factor $S(k)$ was calculated directly, using

$$S(k) = N_c^{-1}\langle\rho(\boldsymbol{k})\rho(-\boldsymbol{k})\rangle \qquad \text{where } \rho(\boldsymbol{k}) = \sum_{i=1}^{N_c}\exp(\mathrm{i}\boldsymbol{k}\cdot\boldsymbol{R}_i).$$

In figures 2–8, we show $g(r)$ and $S(k)$ for four size ratios at the state-points denoted by the asterisks in figure 1. The packing fractions of the state-points are given in table 1.

We also calculated the structure factor and radial distribution function for the effective one-component system using the Percus–Yevick (PY) closure, which is expected to be accurate for short-ranged pair potentials of the type that we consider here [12]. These results are plotted in the same figures as the simulation results. The overall level of agreement between the PY

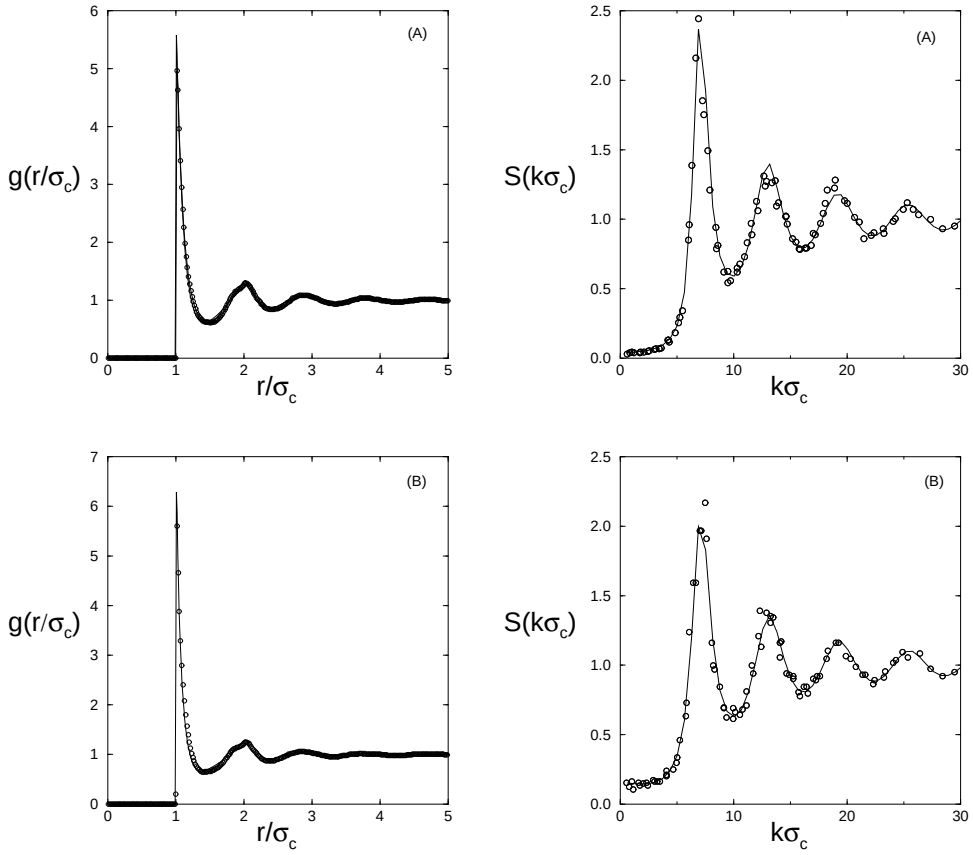

Figure 2. The radial distribution function $g(r/\sigma_c)$ and the structure factor $S(k\sigma_c)$ for the effective one-component system, based on the Asakura–Oosawa pair potential (8), with size ratio $q = 0.4$ at the two different state-points A and B, denoted by the asterisks in figure 1(b) and given in table 1. The solid lines are the PY results and the open circles are those obtained from simulations.

results and those of simulation is remarkably good. The only significant differences are at the first maximum of $S(k)$ (near $2\pi/\sigma_c$), where PY approximation appears to underestimate the height slightly for certain state-points.

For each value of q the state-point A is at $\eta_c \simeq 0.48$ and $\eta_p^r = 0.20$. In each case the effective pair potential is relatively shallow and its range is not very short. Thus we expect to find $g(r)$ and $S(k)$ which are similar to those of the hard-sphere fluid close to freezing and this is what is observed. The attraction has little effect at this large colloid packing fraction. State-point B corresponds to the triple point for $q = 0.6$ and 0.8. η_c remains large but the polymer reservoir packing fraction η_p^r is also large, so the effect of attraction is greater than at points A. This leads to somewhat larger values of $g(\sigma_c)$ and to substantially larger values of $S(k)$ at small k than for hard spheres. Point B for $q = 0.4$ is not a triple point. We shall return to the results for state-points B in section 6 when we make comparison with experiments. State-point C is close to the fluid–fluid critical point for $q = 0.6$ and 0.8 and lies slightly below the metastable critical point for $q = 0.4$. In all three cases $S(k)$ exhibits a steep rise as $k \to 0$, characteristic of Ornstein–Zernike behaviour. The small-angle scattering appears to be just as pronounced for $q = 0.4$, for which the point C is separated from the metastable critical

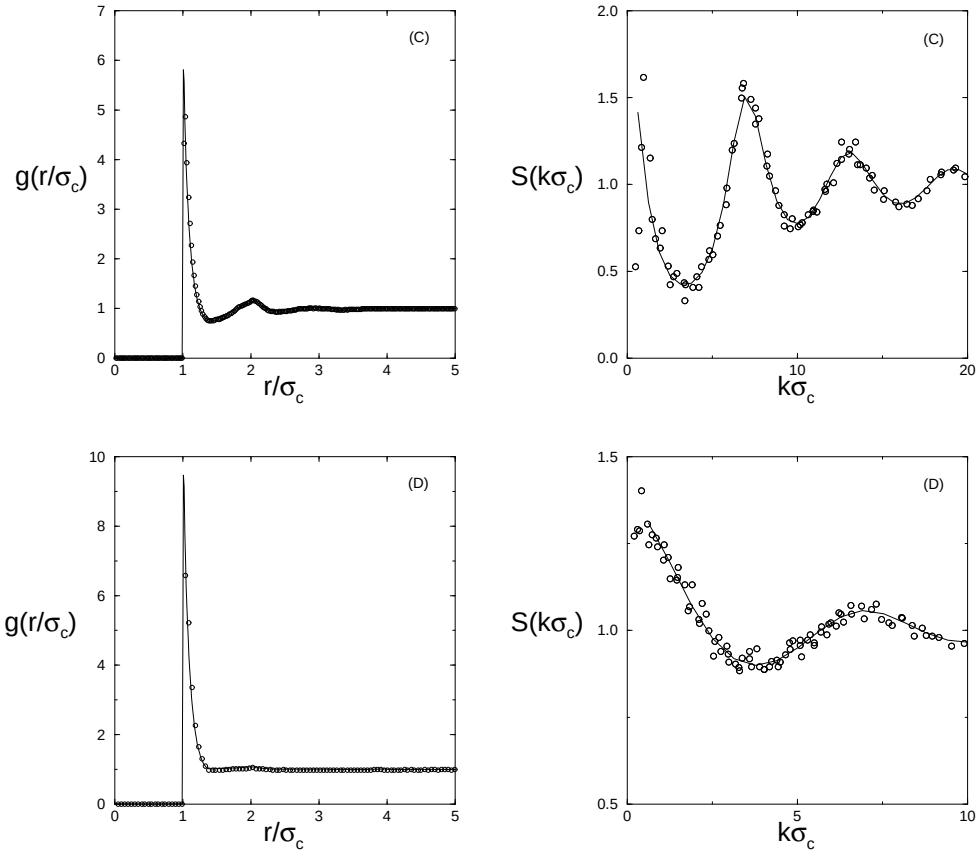

Figure 3. The radial distribution function $g(r/\sigma_c)$ and the structure factor $S(k\sigma_c)$ for the effective one-component system, based on the Asakura–Oosawa pair potential (8), with size ratio $q = 0.4$ at the two different state-points C and D, denoted by the asterisks in figure 1(b) and given in table 1. The solid lines are the PY results and the open circles are those obtained from simulations.

point by the solid–fluid boundary, as for $q = 0.6$ and 0.8, where the critical points are stable. The situation is very different for $q = 0.1$. Here state-point C lies close to the solid–fluid boundary but is far removed from the metastable critical point. Figure 8 shows that there is no increase in $S(k)$ at small k for this state. It is important to note that the PY results capture the Ornstein–Zernike behaviour, when it occurs, as well as all the other features in $S(k)$ and $g(r)$. This suggests that the PY approximation should yield critical points in the neighbourhood of those found in simulation.

State-points D correspond to very dilute colloid packing, i.e. $\eta_c = 0.02$. They lie on the 'gas' side of the fluid–fluid coexistence curve for $q = 0.6$ and 0.8, and, for $q = 0.4$, point D is very close to the fluid–solid phase boundary. The pair potential is strongly attractive since η_p^r is 0.6 or 0.5. As the colloid density is very low the maxima in $S(k)$ are much reduced in comparison to other state-points. The pronounced increase in $S(k)$ at small k is found for similar low-density states of the rare-gas fluids Ar, Kr etc [20]. It reflects the fact that the compressibility is large, due to the influence of attractive interactions, giving rise to $S(0) > 1$. The contact values $g(\sigma_c)$ are also large, and they increase with decreasing size ratio. This trend can be attributed to the fact that the well depth $-\phi_{\mathrm{AO}}(\sigma_c)$ increases as q decreases and

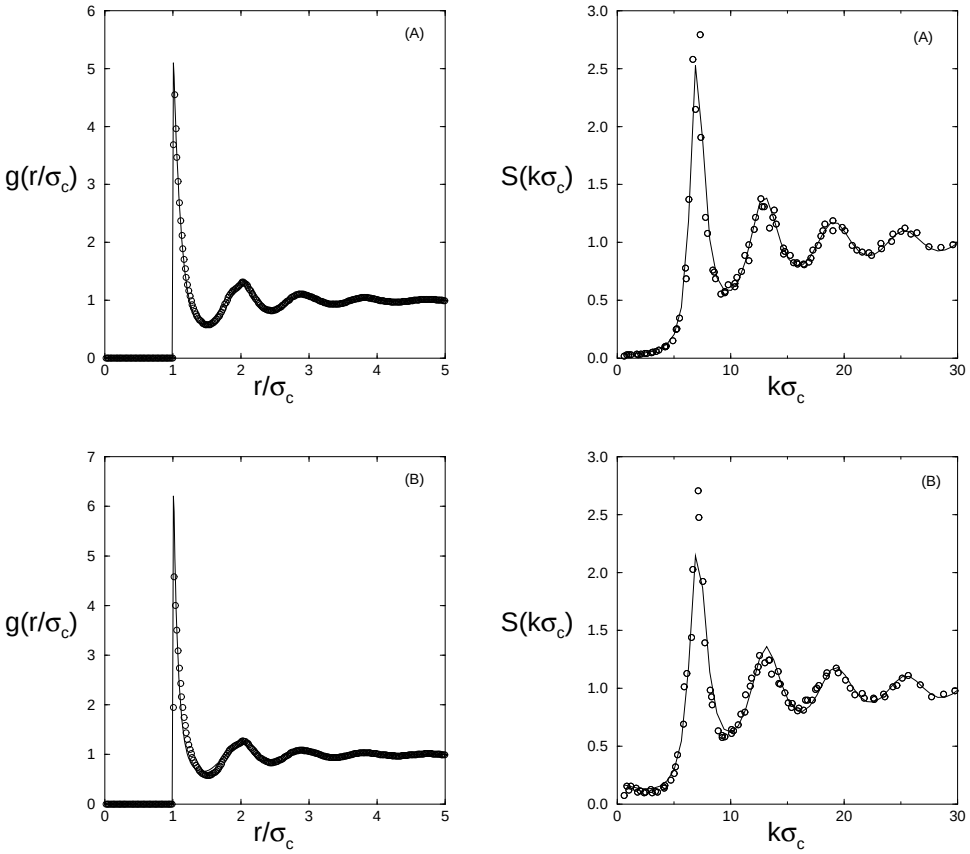

Figure 4. The radial distribution function $g(r/\sigma_c)$ and the structure factor $S(k\sigma_c)$ for the effective one-component system, based on the Asakura–Oosawa pair potential (8), with size ratio $q = 0.6$ at the two different state-points A and B, denoted by the asterisks in figure 1(c) and given in table 1. The solid lines are the PY results and the open circles are those obtained from simulations.

that $g(r) \sim \exp(-\beta\phi_{\rm eff}(r))$ for these low densities. Note that $g(r)$ decays to a value close to unity over the range (σ_p) of $\phi_{\rm eff}(r)$, i.e. the clustering of the colloids is confined to this range.

The structure factors for $q = 0.4$ reinforce the observation made in earlier work [11] that the Hansen–Verlet [13] freezing criterion is not universally applicable. Points D and C lie close to the fluid–solid phase boundary but the heights of the first maximum $S(k_m)$ are 1.06 and 1.6, respectively. These values are far below the value 2.85 required by the one-phase freezing criterion. The latter is somewhat more reliable for points B and A. But there the colloid packing fraction $\eta_c \geqslant 0.43$, so one expects to have fairly large values of $S(k_m)$. For $q = 0.6$ and 0.8 freezing occurs for high values of η_c and the criterion appears to be obeyed.

Recently Vliegenthart *et al* [21] have performed computer simulations of the phase behaviour and structure factor of models with Lennard-Jones $2n - n$ pairwise potentials. For $n \geqslant 11$ the potential is sufficiently short ranged that the fluid–fluid coexistence becomes metastable with respect to fluid–solid, i.e. the critical temperature lies below the fluid–solid phase boundary. Several of the features that they find in their structure factors are similar to those that we obtain here.

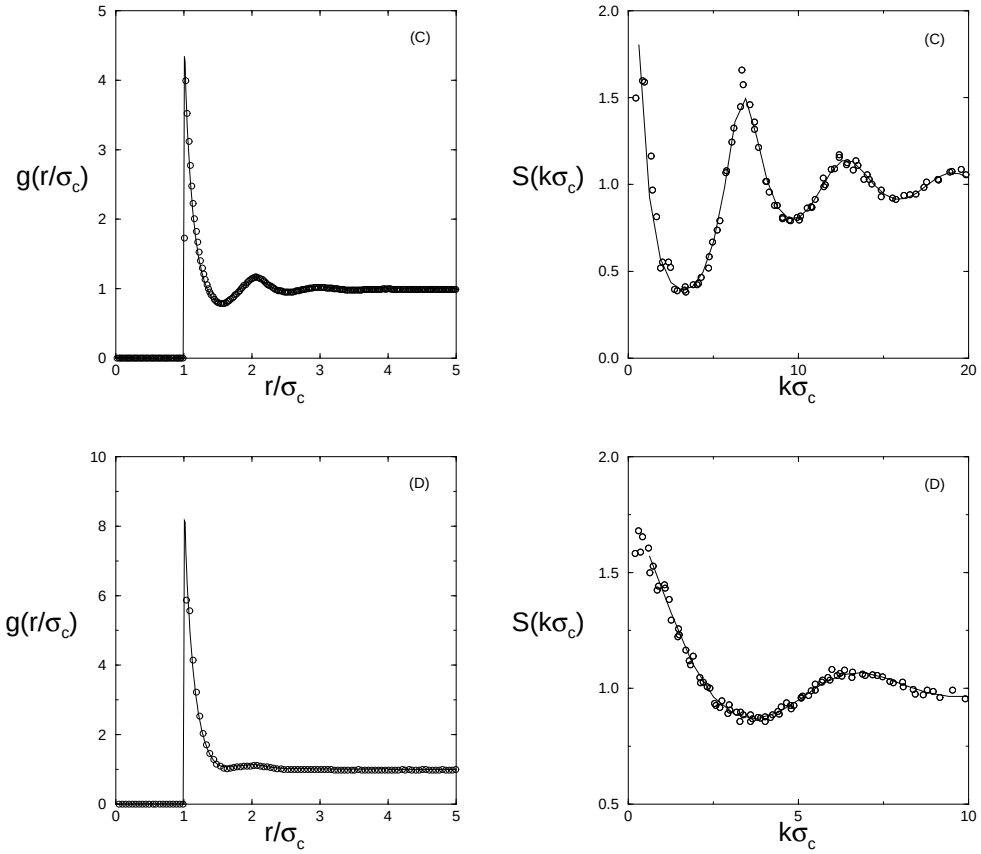

Figure 5. The radial distribution function $g(r/\sigma_c)$ and the structure factor $S(k\sigma_c)$ for the effective one-component system, based on the Asakura–Oosawa pair potential (8), with size ratio $q = 0.6$ at the two different state-points C and D, denoted by the asterisks in figure 1(c) and given in table 1. The solid lines are the PY results and the open circles are those obtained from simulations.

4. Results of approximate theories

In this section we focus on approximate theories of the phase equilibria of colloid–polymer mixtures. Given that we adopted the effective one-component Hamiltonian (9) we can employ standard techniques, e.g. integral equation or perturbative methods. We have already seen from section 3.2 that the PY integral equation theory yields a very good account of the colloid–colloid correlations. However, such theories do not lend themselves so readily to investigations of the phase equilibria; issues of thermodynamic self-consistency become important.

Here we consider first a simpler approach—namely thermodynamic perturbation theory, pioneered by Gast *et al* [3] for the present model.

The second approach is the free-volume theory of Lekkerkerker *et al* [4].

As the performance of these theories had not been fully assessed, either in relation to each other or to the results of simulation, we calculate the phase behaviour predicted by both theories for size ratios $q = 0.1$, 0.4, 0.6, and 0.8 and compare with the results of the previous section.

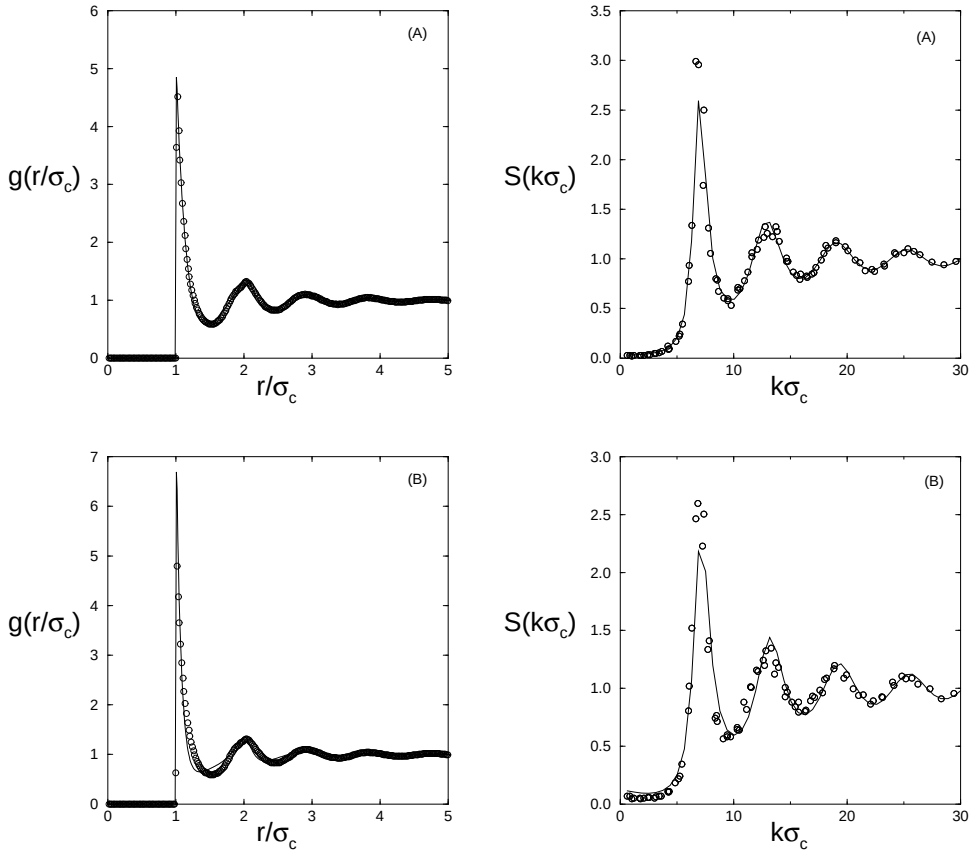

Figure 6. The radial distribution function $g(r/\sigma_c)$ and the structure factor $S(k\sigma_c)$ for the effective one-component system, based on the Asakura–Oosawa pair potential (8), with size ratio $q = 0.8$ at the two different state-points A and B, denoted by the asterisks in figure 1(d) and given in table 1. The solid lines are the PY results and the open circles are those obtained from simulations.

4.1. Perturbation theory

The simplest form of perturbation theory is the so-called high-temperature expansion, which to first order in β gives the Helmholtz free energy of the perturbed system as [12]

$$\frac{\beta F}{N} = \frac{\beta F_0}{N} + \frac{1}{2}\beta\rho \int \mathrm{d}\boldsymbol{r}\; g_0(r)w(r) \tag{12}$$

where F_0 and $g_0(r)$ are the free energy and radial distribution function of the reference system, $\rho \equiv N/V$, and $w(r)$ is the perturbing potential. The second-order terms in the high-temperature expansion involve three- and four-body distribution functions of the reference system, which are in general unknown. However, Barker and Henderson [22] have derived an alternative formulation of the second-order term which involves only two-body correlations and which is much more convenient for practical calculations. When the Barker–Henderson second-order term is included, the free energy is given by

$$\frac{\beta F}{N} = \frac{\beta F_0}{N} + \frac{1}{2}\beta\rho \int \mathrm{d}\boldsymbol{r}\; g_0(r)w(r) - \left(\frac{\partial\rho}{\partial p}\right)_0 \frac{1}{4}\beta\rho \int \mathrm{d}\boldsymbol{r}\; g_0(r)w^2(r). \tag{13}$$

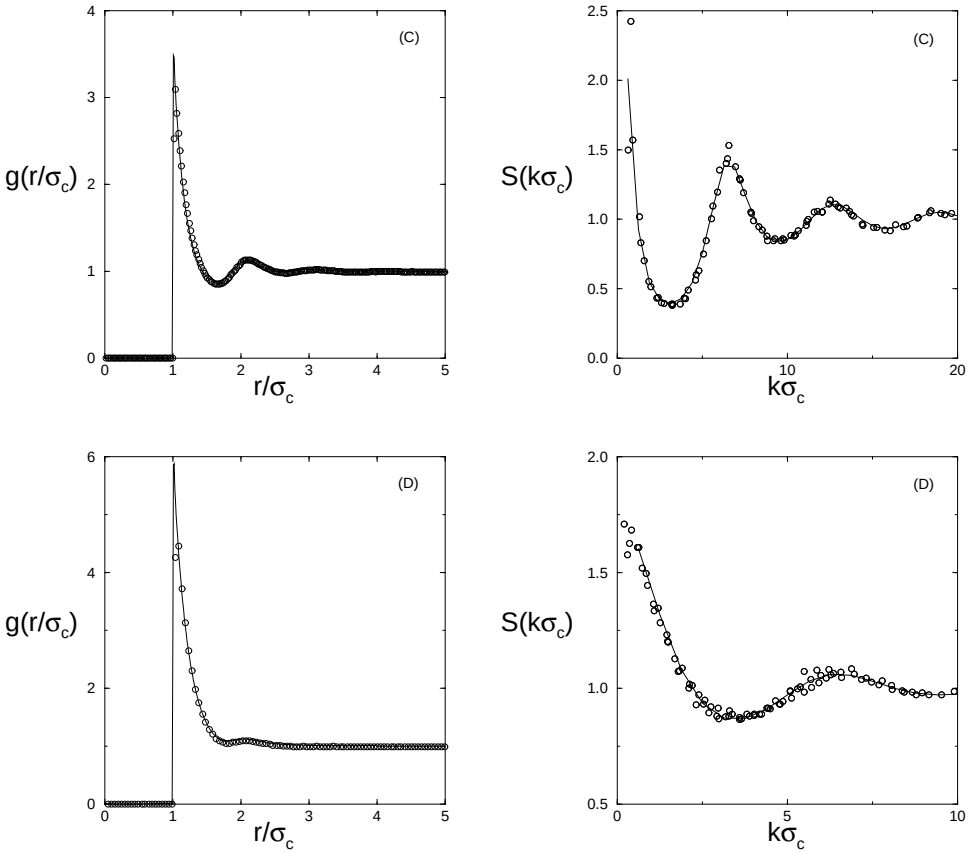

Figure 7. The radial distribution function $g(r/\sigma_c)$ and the structure factor $S(k\sigma_c)$ for the effective one-component system, based on the Asakura–Oosawa pair potential (8), with size ratio $q = 0.8$ at the two different state-points C and D, denoted by the asterisks in figure 1(d) and given in table 1. The solid lines are the PY results and the open circles are those obtained from simulations.

The second-order term is proportional to the compressibility of the reference system and this result is often referred to as the macroscopic compressibility approximation.

The most natural way to calculate the thermodynamic properties of the present system with pairwise potential ϕ_{eff} is to treat ϕ_{AO} as a perturbation and take hard spheres as the reference system. The first such study was due to Gast *et al* [3] who calculated phase diagrams for a selection of size ratios using the second-order expression (13). In order to gain a more complete picture we adopt the same approach and map out the phase diagrams for $q = 0.1$, 0.4, 0.6, and 0.8. In each case the free energy is calculated from (13) and the coexisting densities are determined by the common-tangent construction.

The reference hard-sphere free energies for the fluid and solid phases were provided by the Carnahan–Starling [16] and Hall [17] expressions, respectively and the reference system radial distribution functions used were those of Verlet and Weis [23] for the fluid phase and Kincaid and Weis [24] for the solid. The calculated phase diagrams are given in figure 9 and comparison with the simulation results of figure 1 shows that this perturbation theory gives good overall predictions for the fluid–solid transition, but gives a poor account of the fluid–fluid transition for small q. For $q = 0.6$ and $q = 0.8$, where the effective pair potential is relatively

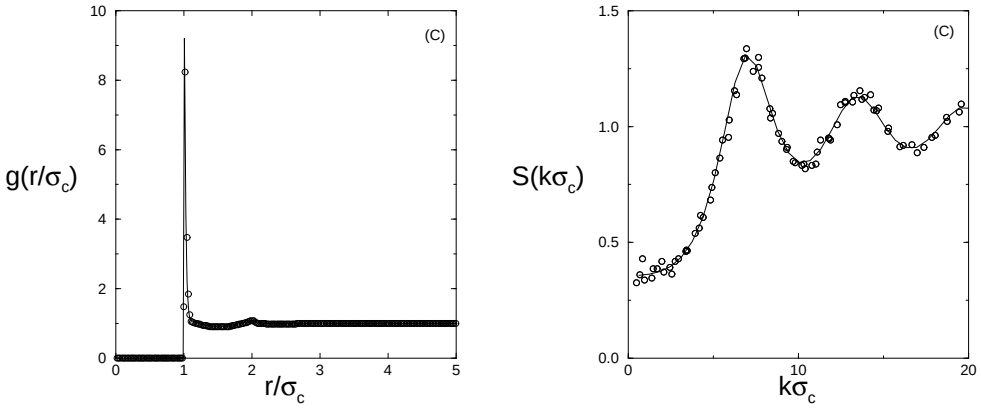

Figure 8. The radial distribution function $g(r/\sigma_c)$ and the structure factor $S(k\sigma_c)$ for the effective one-component system, based on the Asakura–Oosawa pair potential (8), with size ratio $q = 0.1$ at state-point C denoted by the asterisk in figure 1(a) and given in table 1. The solid lines are the PY results and the open circles are those obtained from simulations.

Table 1. The state-points at which the colloid–colloid structure factors and radial distribution functions were determined in terms of the packing fraction η_c of the colloids and the packing fraction η_p^r of polymer coils in the reservoir. These state-points are denoted by asterisks in figure 1.

State-point	η_c	η_p^r
	$q = 0.1$	
C	0.250	0.160
	$q = 0.4$	
A	0.475	0.200
B	0.425	0.400
C	0.240	0.440
D	0.02	0.500
	$q = 0.6$	
A	0.480	0.200
B	0.440	0.600
C	0.230	0.490
D	0.02	0.600
	$q = 0.8$	
A	0.480	0.200
B	0.470	0.730
C	0.210	0.485
D	0.02	0.600

long ranged, the phase diagram resembles that of a simple (e.g. Lennard-Jones) liquid, with η_s^r playing the role of an inverse temperature. In both cases the triple points are in good agreement with those of simulation, and the critical points are at the correct values of η_c but are too low in η_p^r. For $q = 0.4$ the triple and critical points lie close to one another, but the fluid–fluid transition remains stable for this size ratio. In contrast to the simulation results, which show

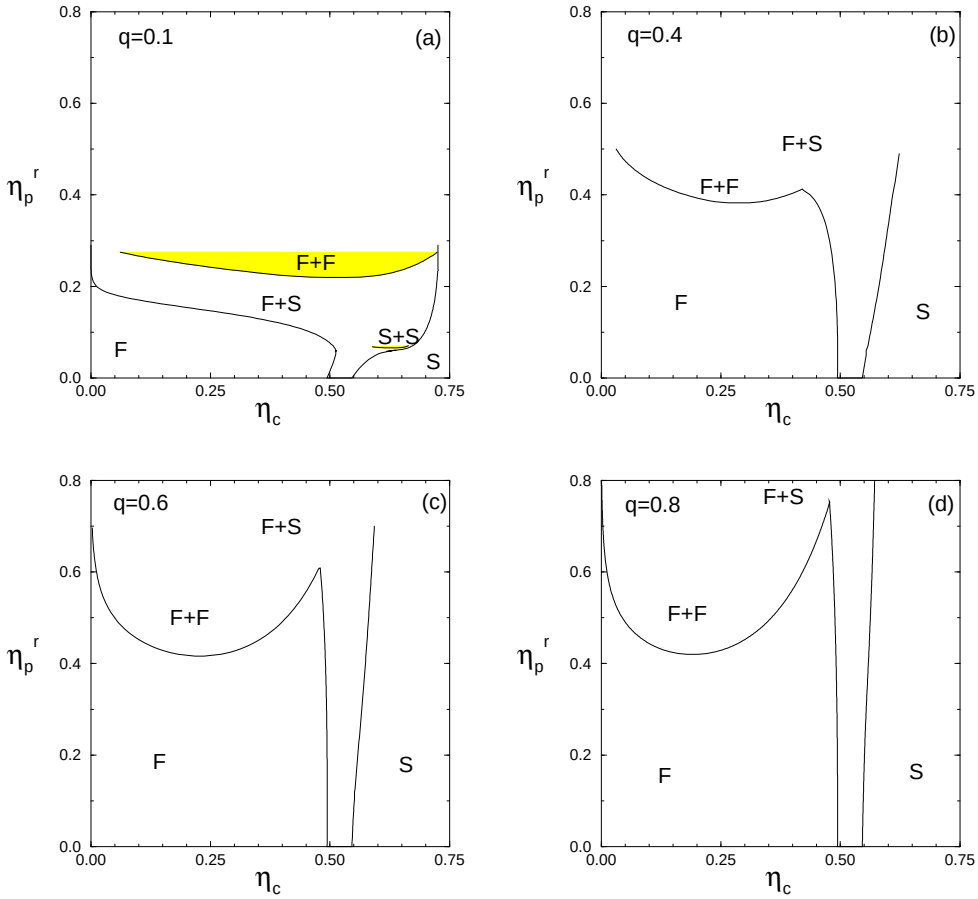

Figure 9. Phase diagrams of model colloid–polymer mixtures as obtained from perturbation theory of the effective one-component Hamiltonian with size ratios (a) $q = \sigma_p/\sigma_c = 0.1$, (b) $q = 0.4$, (c) $q = 0.6$, and (d) $q = 0.8$ as functions of the colloid packing fraction η_c and the ideal polymer coil reservoir packing fraction η_p^r. F and S denote the stable fluid and solid (fcc) phase. F + S, F + F, and S + S denote, respectively, the stable fluid–solid, the (meta)stable fluid–fluid, and the metastable solid–solid coexistence region.

that the fluid–fluid transition becomes metastable for $q \leqslant 0.45$, the perturbation theory yields a crossover value of $q \sim 0.31$. For $q = 0.1$ the fluid–solid phase boundary becomes more structured and the melting line flattens for $\eta_p^r \sim 0.08$. An isostructural (FCC–FCC) solid–solid transition is obtained, and, in agreement with the simulation results, this is weakly metastable with respect to the fluid–solid transition. It should be noted that this solid–solid transition was not identified in the original work of Gast *et al* [3]. Perturbation theory gives a good account of the solid–fluid phase boundaries for $q = 0.1$. The only difference lies in the slope of the freezing line at low η_p^r; perturbation theory gives a positive slope whereas simulation yields a negative slope. On the other hand, the perturbation theory fails to predict a realistic fluid–fluid transition for $q = 0.1$. In particular, the critical point is shifted to unphysically high values of η_c, a defect which is found to become even worse as q becomes smaller.

In order to determine the sensitivity of the results to details of the perturbation theory, the effect of using different expressions for the hard sphere $g_0(r)$ was investigated. The two

expressions used were the Percus–Yevick result and the more accurate empirical result of Verlet and Weis. We find that while the fluid–solid transition is largely unaffected by the choice of $g_0(r)$, the fluid–fluid phase boundary is quite sensitive. Using the Verlet–Weis expression moves the critical point to lower η_p^r-values, an effect which becomes more pronounced at smaller q-values. The main difference between the Percus–Yevick and the Verlet–Weis expressions is that the Percus–Yevick one underestimates the contact value $g_0(\sigma_c)$. As $\phi_{\rm AO}$ is deepest at contact, any variation in $g_0(\sigma_c)$ is heavily weighted in the perturbation integrals and so affects the phase behaviour accordingly. We also investigated the effect of omitting the Barker–Henderson second-order term. We find that this alters the value of the free energy by typically less than five per cent. The effect on the phase boundaries is found to be negligible for the fluid–solid and small for the fluid–fluid transition. In other words, first-order perturbation theory leads to essentially the same results as the second-order results given in figure 9.

4.2. Free-volume theory

A second, alternative approach to calculating the phase behaviour of colloid–polymer mixtures was proposed by Lekkerkerker *et al* [4]. While this can be viewed as a type of perturbation expansion, its basis is very different from the approach described above. It does not work from the outset with the effective Hamiltonian (9), i.e. the Asakura–Oosawa pair potential does not appear explicitly. Rather than following the original presentation of the theory [4] we give an alternative treatment which clarifies the status of the various approximations. Consider the thermodynamic identity

$$\beta F(N_c, V, z_p) = \beta F(N_c, V, z_p = 0) + \int_0^{z_p} \mathrm{d}z_p' \left(\frac{\partial \beta F(N_c, V, z_p')}{\partial z_p'} \right) \tag{14}$$

where z_p is, as usual, the polymer fugacity. The integrand can now be Taylor expanded about $z_p = 0$:

$$\beta F(N_c, V, z_p) = \beta F(N_c, V, z_p = 0) + z_p \left(\frac{\partial \beta F(N_c, V, z_p)}{\partial z_p} \right)_{z_p=0} + \mathcal{O}(z_p^2). \tag{15}$$

The partial derivative can be obtained from equations (3) and (5) and is given by

$$-\left(\frac{\partial \beta F(N_c, V, z_p)}{\partial z_p} \right)_{z_p=0} = \mathrm{Tr}_c \left(\exp[-\beta H_{cc}] \int \mathrm{d}\boldsymbol{r}_j \prod_{i=1}^{N_c} (1 + f_{ij}) \right) \Big/ \mathrm{Tr}_c \exp[-\beta H_{cc}] \tag{16}$$

where Tr_c is short for the integral $\int_V \mathrm{d}\boldsymbol{R}^{N_c}$ over the coordinates of the colloidal particles. Due to the form of the Mayer function f_{ij} for the colloid–polymer interaction, equation (16) can be interpreted as the average free volume available to a polymer coil in a system of N_c colloids when $z_p = 0$. Equation (15) can be rewritten as

$$\beta F(N_c, V, z_p) = \beta F(N_c, V, z_p = 0) - z_p \langle V_{\rm free} \rangle_{z_p=0} + \mathcal{O}(z_p^2). \tag{17}$$

This derivation follows that of [11] where an identical expression is derived for the additive binary hard-sphere mixture. As the polymer is ideal, z_p can be replaced by $\beta p^r(z_p)$, where $p^r(z_p)$ is the pressure of the reservoir. In contrast to the binary hard-sphere case [11], this replacement is exact. The free-volume theory [4] retains only the first-order term, neglecting terms $\mathcal{O}(z_p^2)$ and higher. With this assumption, equation (17) can be written as the sum of two terms:

$$F(N_c, V, z_p) = F_0(N_c, V) - p^r(z_p) \alpha V \tag{18}$$

where $\alpha \equiv \langle V_{\text{free}} \rangle_{z_p=0}/V$ is the free-volume fraction of a test polymer in the colloidal system with packing fraction η_c. The first term is the Helmholtz free energy F_0 of a pure hard-sphere fluid at the given η_c, while the second can be interpreted as the grand potential of ideal polymers free to occupy a volume αV. All information about the interactions between colloid and polymer is now contained in the variation of α with η_c. As previously, the Carnahan–Starling or Hall expressions are used for F_0 in the fluid and solid phases, respectively. An approximate expression for α can be obtained by use of scaled-particle results (see [4]) which give

$$\alpha = (1 - \eta_c)\ \exp(-A\gamma - B\gamma^2 - C\gamma^3) \tag{19}$$

where $\gamma = (\eta_c)/(1 - \eta_c)$, $A = 3q + 3q^2 + q^3$, $B = 9q^2/2 + 3q^3$, and $C = 3q^3$. The chemical potential μ_c and total osmotic pressure Π can now be found by differentiation:

$$\mu_c = \left(\frac{\partial F}{\partial N_c}\right)_{V,z_p} = \mu_0(\eta_c) - p^r(z_p)\left(\frac{\mathrm{d}\alpha}{\mathrm{d}\eta_c}\right)\pi\sigma_c^3/6 \tag{20}$$

$$\Pi = -\left(\frac{\partial F}{\partial V}\right)_{N_c,z_p} = p_0(\eta_c) + p^r(z_p)\left(\alpha - \eta_c\left(\frac{\mathrm{d}\alpha}{\mathrm{d}\eta_c}\right)\right) \tag{21}$$

where μ_0 and p_0 are the chemical potential and pressure of the hard-sphere fluid. The volume fractions of the colloidal particles in each of the coexisting phases, η_c^1 and η_c^2, are obtained by equating μ_c and Π at fixed η_p^r.

In order to assess the performance of the free-volume theory, phase diagrams were calculated for the same size ratios $q = 0.1$, 0.4, 0.6, and 0.8 as in our previous calculations. The results are shown in figure 10. For $q = 0.4$ the value of η_c at the critical point is in rather good agreement with the previous perturbation theory result but the free-volume theory predicts the fluid–fluid transition to be more strongly stable. Nevertheless we find that for $q \leqslant 0.32$ the fluid–fluid transition becomes metastable with respect to a broad fluid–solid transition. It is surprising that the two theories should give similar results for the q-value at which metastability first occurs, as they follow quite independent routes. However, neither theory agrees with the simulation prediction of metastability at $q \leqslant 0.45$. The solid–fluid 'chimney' for $q = 0.4$ does not exhibit the rapid broadening with increasing η_p^r that is seen in the simulation and perturbation theory results. For $q = 0.1$, the melting line does not flatten out as much as in perturbation theory or simulation. On the other hand, the slope of the freezing line for small η_p^r is given correctly by the free-volume approach. In contrast with simulation and perturbation theory, no solid–solid transition was found in the free-volume approach. However, we do find a spinodal instability in the solid phase, but this instability is very broad and disappears in the fluid phase. We were therefore not able to find a metastable solid–solid coexistence using the common-tangent construction. The fluid–fluid transition again shifts to unphysically high η_c but in an even more extreme way than in perturbation theory, with a critical point at $\eta_c \sim 0.55$. The comparisons for $q = 0.1$ have special importance as this is an example of a mixture, with $q \leqslant 0.154$, where the mapping to the effective one-component Hamiltonian is exact. Thus our simulations should determine, to within statistical accuracy, the 'exact' phase equilibria of the binary mixture. It is significant, therefore, that the free-volume theory fails to capture quantitatively some of the features of the simulation results, i.e. the shape of the melting line and the development of the solid–solid transition. For $q = 0.6$ the free-volume theory yields a fluid–fluid critical point quite close to that of simulation and perturbation theory. The solid–fluid 'chimney' remains unbroadened, however, leading to a triple point at $\eta_p^r \sim 1.37$ whereas the simulation value is at about 0.60. This trend is maintained for $q = 0.8$ where the free-volume estimate of η_p^r at the triple-point increases to $\sim$3.21, while our simulation

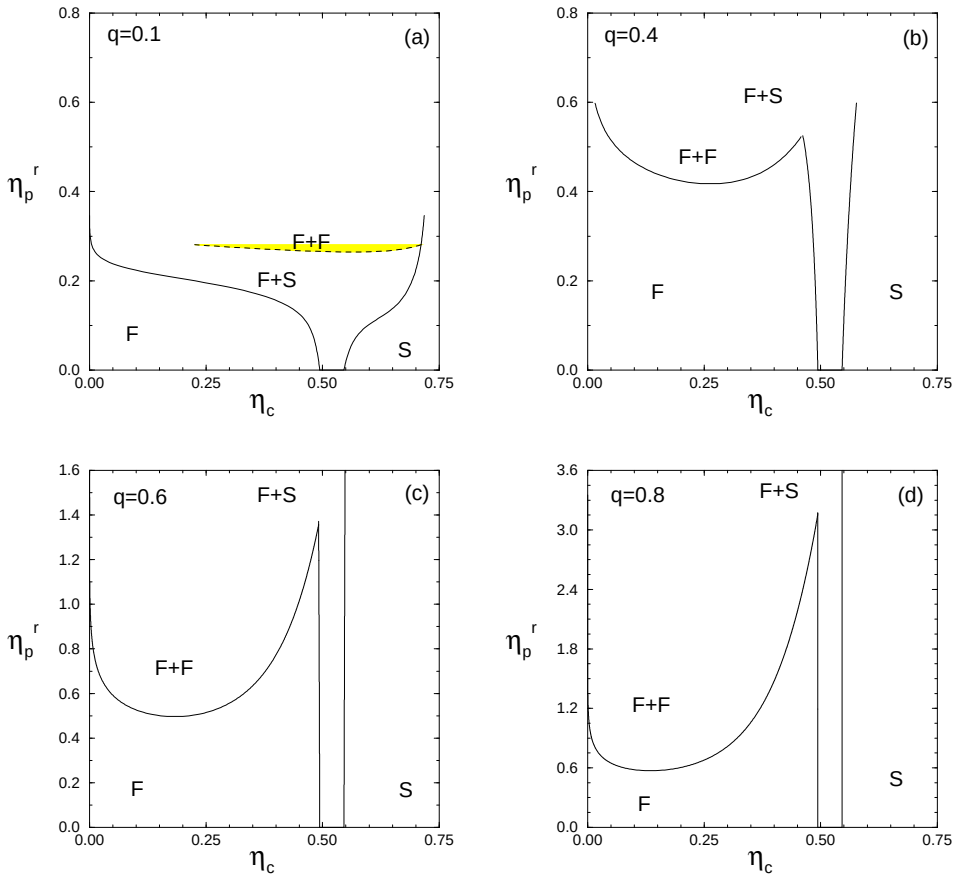

Figure 10. Phase diagrams of model colloid–polymer mixtures as obtained from the free-volume approach with size ratios (a) $q = \sigma_p/\sigma_c = 0.1$, (b) $q = 0.4$, (c) $q = 0.6$, and (d) $q = 0.8$ as functions of the colloid packing fraction η_c and the ideal polymer coil reservoir packing fraction η_p^r. F and S denote the stable fluid and solid (fcc) phase. F + S and F + F denote, respectively, the stable fluid–solid and the (meta)stable fluid–fluid coexistence region. Note the difference in scale of η_p^r for $q = 0.6$ and 0.8.

gives the value 0.73. Note that since the polymer is assumed ideal there is no constraint on the values of η_p^r within the model. It is, of course, more difficult to assess the accuracy of the free-volume theory for large values of q. In this regime three-body and higher-body potentials will certainly play a role and these are not incorporated in the present simulations or in the perturbation theory. Some many-body effects are incorporated into the free-volume approach as the free volume, given by (16), does include the effects of higher-order interactions.

Returning to the failings of free-volume theory for $q \leqslant 0.154$, we see that these must be attributed to the neglect of $\mathcal{O}(z_p^2)$ and higher-order terms. We can rewrite the exact expression (14) as

$$\beta F(N_c, V, z_p) = \beta F(N_c, V, z_p = 0) - V \int_0^{z_p} \mathrm{d}z_p' \, \alpha(z_p', \eta_c) \tag{22}$$

where $\alpha(z_p, \eta_c) \equiv \eta_p(z_p, \eta_c)/\eta_p^r$ is the ratio of densities of the polymers in the binary mixture to that in the reservoir, for given fugacity z_p and packing fraction η_c of the colloids. More

precisely, $\eta_p(z_p, \eta_c) = \langle N_p \rangle_{z_p} \pi \sigma_p^3 / 6V$ where $\langle N_p \rangle_{z_p}$ denotes the average number of polymers in the (N_c, V, z_p) ensemble. If $\alpha(z_p, \eta_c)$ is replaced by its low-density limit $\alpha(0, \eta_c) \equiv \alpha$, we recover (18). In reality, however, the free-volume fraction is not independent of z_p; there is no reason to expect the polymer packing fraction η_p to increase linearly with the reservoir fraction η_p^r at fixed η_c. In the case of additive binary hard-sphere mixtures, simulation studies showed [11] that significant deviations from linearity do occur for $q = 0.10$, even at small values of the reservoir packing fraction, when the packing fraction of the big spheres becomes substantial. Small changes in $\alpha(z_p, \eta_c)$ can have a dramatic effect on the phase equilibria since derivatives of this fraction with respect to η_c determine the conditions for coexistence. It is not obvious how to improve systematically upon the basic approximation which sets $\alpha(z_p, \eta_c)$ equal to its value at $z_p = 0$.

5. Connection with additive binary hard-sphere mixtures

In this section we shift our attention to the additive binary hard-sphere mixture, which is closely related to the Asakura–Oosawa model considered previously. Once more we adopt an effective one-component Hamiltonian and calculate the phase equilibria using thermodynamic perturbation theory as in section 4.1. The motivation for this investigation is firstly to determine the accuracy of the perturbation theory by comparing the results with those of recent computer simulations of the binary mixture [11] for $q = 0.1$ and $q = 0.2$, and secondly to compare the evolution of the phase diagram as q is reduced with that of the Asakura–Oosawa model in order to identify any common trends or significant differences.

5.1. Phase diagrams obtained from the depletion potential

The binary hard-sphere model consists of a mixture of large and small hard spheres with diameters σ_1 and σ_2, respectively, and with size ratio $q = \sigma_2/\sigma_1$. For the additive case the pair potential between species 1 and 2 is described by a diameter $\sigma_{12} = (\sigma_1 + \sigma_2)/2$. Theoretical studies of the phase equilibria for small q have been largely inconclusive, particularly with regard to the existence of a fluid–fluid demixing transition. However, recent simulations [11] have resolved this issue and shown that although a fluid–fluid transition does occur for small q, this remains metastable with respect to a broad fluid–solid transition. The simulation study also found stable solid–solid transitions at very small size ratios [11]. Here we adopt the same strategy as in section 2 and in reference [11], i.e. we take advantage of the size asymmetry of the problem and integrate out the degrees of freedom of the small spheres. The resulting effective Hamiltonian consists of zero-body, one-body, two-body, and many-body terms. As in reference [11] we retain only the two-body contribution and neglect all higher-body interactions. The pair potential can, once again, be identified with the depletion potential between two large spheres in a sea of small particles. In the present case the depletion potential is more complicated than that for ideal small particles, where it is simply the Asakura–Oosawa potential (8), and there are no exact results available for arbitrary q and η_2^r. We use an approximation given by Götzelmann *et al*, which provides an excellent fit to simulation results for the depletion potential for two hard spheres in a sea of small hard spheres for $q = 0.1$ and reservoir packing fractions η_2^r as large as 0.34 [25]. The same potential was employed in [11] as it has a simple (polynomial) form:

$$\beta\phi_{\mathrm{dep}}(R_{ij}) = -\frac{1+q}{2q}(3x^2\eta_2^r + (9x + 12x^2)(\eta_2^r)^2 + (36x + 30x^2)(\eta_2^r)^3) \qquad \text{for } -1 < x < 0 \tag{23}$$

where

$$x = R_{ij}/\sigma_2 - 1/q - 1.$$

Contact corresponds to $R_{ij} = \sigma_1$ or $x = -1$. The total effective pair potential is $\phi_{\rm eff} = \phi_{11} + \phi_{\rm dep}$, where ϕ_{11} is the hard-sphere potential between two large spheres. Examples of $\phi_{\rm dep}$ and comparisons with $\phi_{\rm AO}$ are given in figures 11 and 12. For simplicity we set $\phi_{\rm dep} = 0$ for $R_{ij} > \sigma_1 + \sigma_2$, i.e. it has the same range as $\phi_{\rm AO}$. In reality the (hard-sphere) depletion potential exhibits exponentially damped oscillations as $R_{ij} \to \infty$ [26] but these should not be important for the phase behaviour. The key difference between $\phi_{\rm dep}$ and $\phi_{\rm AO}$ is the development in the former of a repulsive barrier, whose height increases with increasing η_2^r. Note that to first order in η_2^r, equation (23) reduces to the Asakura–Oosawa potential (8) evaluated in the so-called Derjaguin approximation (valid for $q \to 0$) [25]. It should

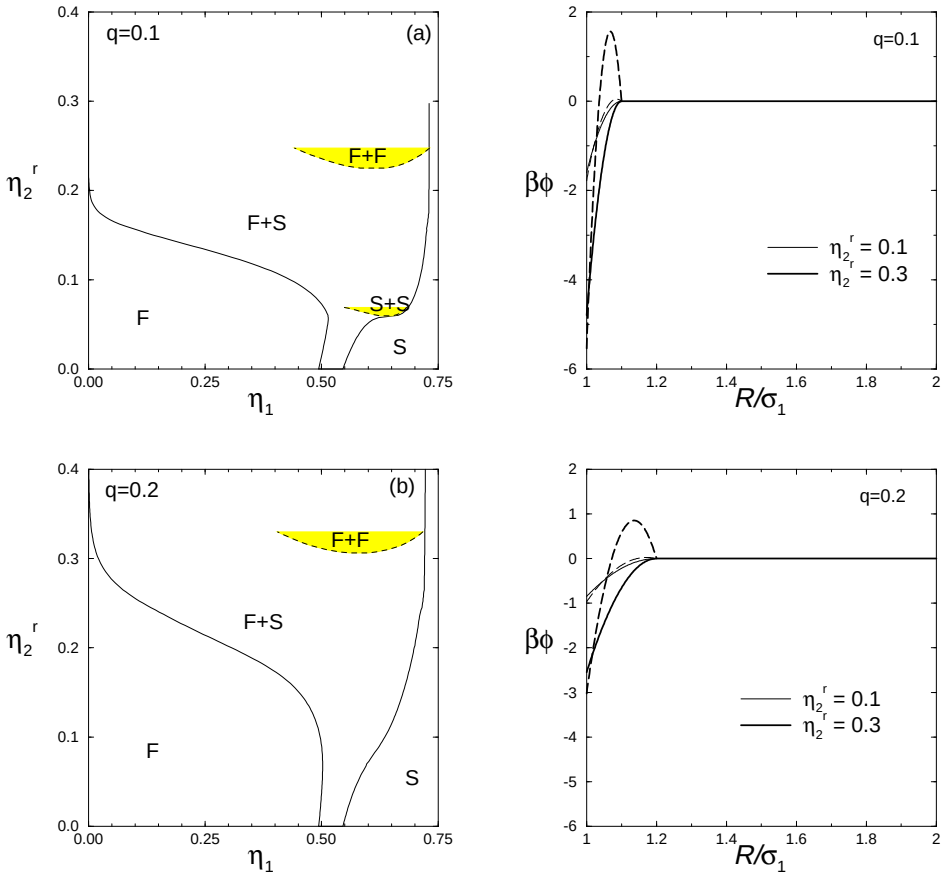

Figure 11. Phase diagrams of additive binary hard-sphere mixtures with size ratios (a) $q = \sigma_2/\sigma_1 = 0.1$, and (b) $q = 0.2$, as functions of the large-sphere packing fraction η_1 and the small-sphere reservoir packing fraction η_2^r as obtained from the perturbation theory of the effective one-component Hamiltonian. F and S denote the stable fluid and solid (fcc) phase. F + S, F + F, and S + S denote, respectively, the stable fluid–solid, the (meta)stable fluid–fluid, and the metastable solid–solid coexistence region. The effective pair potentials for the additive binary hard-sphere mixture (dashed lines) and the Asakura–Oosawa pair potential (solid lines) for the colloid–polymer mixture are shown together on the right-hand side for $\eta_2^r = 0.1$ (faint) and 0.3 (bold).

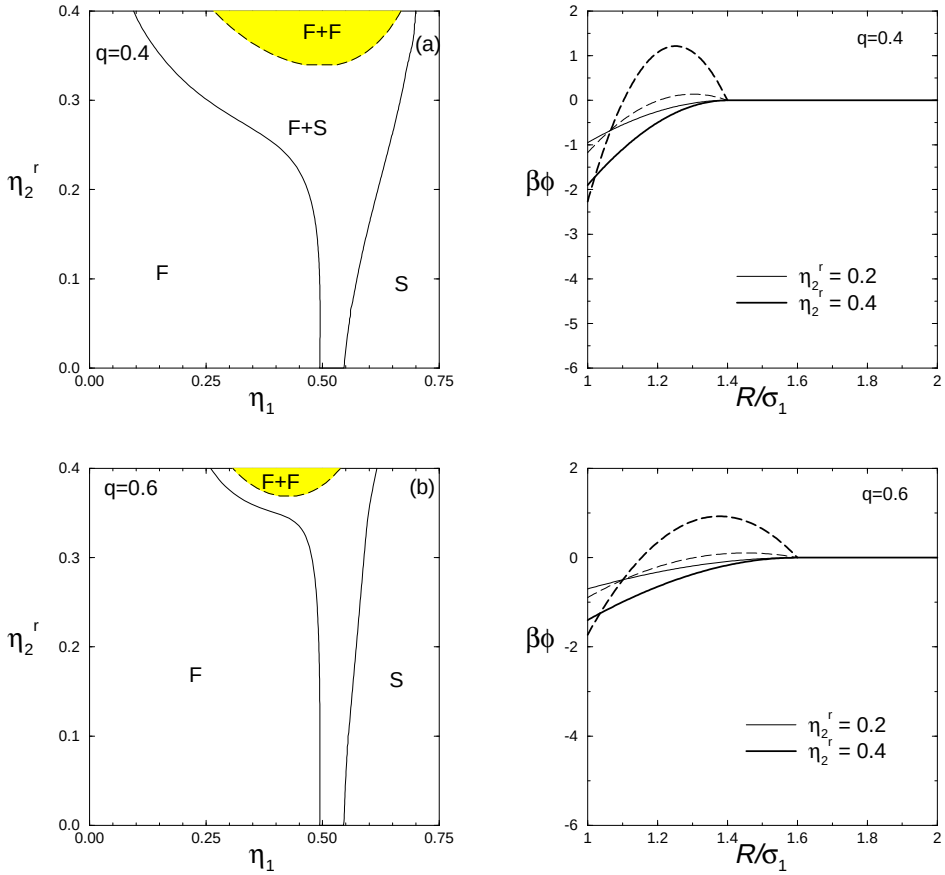

Figure 12. Phase diagrams of additive binary hard-sphere mixtures with size ratios (a) $q = \sigma_2/\sigma_1 = 0.4$, and (b) $q = 0.6$, as functions of the large-sphere packing fraction η_1 and the small-sphere reservoir packing fraction η_2^r as obtained from the perturbation theory of the effective one-component Hamiltonian. F and S denote the stable fluid and solid (fcc) phase. F + S and F + F denote, respectively, the stable fluid–solid and the metastable fluid–fluid coexistence region. The effective pair potentials for the additive binary hard-sphere mixture (dashed lines) and the Asakura–Oosawa pair potential (solid lines) for the colloid–polymer mixture are shown together on the right-hand side for $\eta_2^r = 0.2$ (faint) and 0.4 (bold).

be emphasized once more that in this additive case there is no *exact* mapping between the partition functions of the full binary system and the effective one-component system, even for $q \leqslant 0.154$, because the interactions between the small spheres can still mediate many-body forces. Nevertheless, comparison with the results of direct simulations of the true binary hard-sphere mixture showed that the effective (two-body) Hamiltonian provides an accurate description of the fluid–solid phase boundary for size ratios $q = 0.2$, 0.1, and 0.05 and of the solid–solid boundary for $q = 0.1$ and 0.05 [11]. This implies that the higher-body terms, omitted in the effective-pairwise-depletion approximation, do not play an important role for the additive hard-sphere case.

In order to calculate the phase behaviour we adopt the second-order perturbation theory used in section 4, treating the pair potential (23) as the perturbation with hard spheres as the reference. The calculated phase diagrams are shown in figures 11 and 12 as functions of the

large-sphere packing fraction η_1 and the small-sphere reservoir packing fraction η_2^r†. Our results for $q = 0.1$ and $q = 0.2$ can be compared directly with the simulation results of reference [11]. We find that the perturbation theory provides a good overall account of the solid–fluid transition. As was the case for the Asakura–Oosawa potential, the only noticeable difference lies in the slope of the freezing line at low η_2^r; whereas perturbation theory indicates that this is positive, the simulations suggest that it is negative. Perturbation theory yields a metastable solid–solid transition for $q = 0.1$ similar to that found in simulation. The critical point of this transition continues to lie very close to the fluid–solid phase boundary as q is reduced to below 0.1, and the transition may even become stable for sufficiently small q-values, again in agreement with the simulation [11]. As was the case for the model colloid–polymer mixture, perturbation theory gives a very poor account of the (metastable) fluid–fluid transition. For $q = 0.1$ this occurs at unphysically large values of η_1; the critical point is near $\eta_1 = 0.6$, whereas simulation gives $\eta_1 \sim 0.25$ [11]. When q increases to 0.2 the metastable fluid–fluid critical point shifts to a slightly lower value $\eta_1 \simeq 0.56$ and a reservoir packing fraction $\eta_2^r \simeq 0.31$. In simulation, however, there is no indication of the fluid–fluid transition for this particular size ratio; it has shifted to very high (unphysical) values of η_2^r [11]. Simulation results are not available for $q = 0.4$ and 0.6 but we note that for $q = 1$ there is no fluid–fluid transition. As q is increased, the fluid–fluid critical point moves to lower η_1 but to only slightly higher η_2^r. Indeed the fluid–fluid transition is predicted to be only weakly metastable for $q = 0.6$ but we believe that this is an artifact of the perturbation theory. In reality the transition should have already disappeared at $q = 0.2$.

5.2. Comparison with results of the Asakura–Oosawa model

The phase diagrams shown in figures 11 and 12 can be compared with those from simulation (figure 1) and from perturbation theory (figure 9) for the Asakura–Oosawa effective pair potential. Comparison with the latter is more straightforward as both sets of results are obtained from the same theoretical framework. For each value of q the phase diagrams in figures 11 and 12 are accompanied by a plot of the corresponding Götzelmann and Asakura–Oosawa effective pair potentials, each given at two different values of η_2^r. For small values of η_2^r the two potentials are very similar, but as η_2^r increases the repulsive barrier develops in the Götzelmann potential and the well depth is deeper than that of the Asakura–Oosawa potential. The phase diagrams for $q = 0.1$ show striking similarities. The fluid–solid and solid–solid phase boundaries of the two models are very close. As mentioned in section 3, the main reason for this is that for $q = 0.1$ most of the interesting phase behaviour occurs at low values of η_2^r and in this region the two depletion potentials are quite similar. The solid–solid critical point lies slightly lower in η_2^r for the Götzelmann potential which is a result of the less attractive tail, as the solid phase $g_0(r)$ gives more weight to the tail of the potential in the perturbation integrals. The broadening of the fluid–solid transition occurs marginally faster with increasing η_2^r for the Götzelmann potential than for the Asakura–Oosawa potential. This reflects the greater well depth of the Götzelmann potential, as the fluid phase $g_0(r)$ gives the contact value of the potential more weight in the perturbation integrals and so initiates the broadening at lower η_2^r than for the Asakura–Oosawa potential.

The fluid–fluid transition is very different in the two models as the depletion potentials differ considerably for the relevant (high) values of η_2^r. As q is increased the phase diagrams

† We note that E Velasco, G Navascués and L Mederos (private communication) have investigated the phase behaviour of additive binary hard-sphere mixtures for small q using the same Götzelmann *et al* effective pair potential. While their perturbation theory approach differs from the present one in the treatment of the hard-sphere reference $g_0(r)$ in the solid, all of their phase boundaries are very close to those that we calculate for $q = 0.1$ and 0.2.

from the two models take on very different appearances. For the Asakura–Oosawa case the fluid–fluid transition becomes stable whereas for the additive binary hard-sphere mixture this is not the case. Given the vast differences in shape between the two types of depletion potential for large η_2^r, it is not surprising that the two models exhibit very different trends in their phase behaviour as a function of q. The Asakura–Oosawa pair potential is attractive and becomes longer ranged as q increases and this can stabilize the fluid–fluid transition. By contrast the depletion potential for the hard-sphere mixture has only a short-ranged attractive contribution before the repulsive barrier takes over, and such potentials are not conducive to a fluid–fluid transition. That the latter occur at all, albeit as metastable transitions, is, as we mentioned above, an artifact of the perturbation theory.

6. Discussion

In this paper we study *both* the phase behaviour and the pair correlation functions for the Asakura–Oosawa model of colloid–polymer mixtures. As direct simulation of the Asakura–Oosawa model is prohibited by slow equilibration we derived an explicit effective one-component Hamiltonian by integrating out the degrees of freedom of the polymer coils. Using the two-body, i.e. the Asakura–Oosawa pair potential, approximation to this effective Hamiltonian in computer simulations, we determined the phase behaviour for size ratios $q = 0.1$, 0.4, 0.6, and 0.8. For $q \geqslant 0.6$, we find a stable fluid–solid and a stable fluid–fluid transition. The latter becomes metastable with respect to a broad fluid–solid transition for $q \leqslant 0.4$. For $q = 0.1$, we find an isostructural solid–solid transition, which is also metastable with respect to the fluid–solid transition, but which is very likely to become stable for smaller values of q. To the best of our knowledge this is the first time such a solid–solid transition has been reported for this model system.

We compare the phase diagrams obtained from simulation with those from a perturbation theory treatment of the same one-component Hamiltonian. The topologies of the phase diagrams as functions of q are similar and the perturbation theory gives a reasonably good overall account of the fluid–solid transition and the solid–solid transition. However, it gives a poor account of the fluid–fluid transition for small q. This failure of perturbation theory to describe the fluid phase accurately at small q warrants further investigation. It is clear that the high-temperature approximation (13) underestimates the magnitude of the attractive contribution to the free energy F for strongly attractive short-ranged perturbations of the type encountered here. What is not so obvious is how to make improvements. In addition, the crossover value where the liquid state becomes 'marginal' is estimated to be at $q \sim 0.45$ in the simulations, whereas the perturbation theory yields a crossover value of $q \sim 0.31$.

We also calculate the phase behaviour of the Asakura–Oosawa model within the free-volume approach [4]. This approach incorporates some many-body effects but our simulations are based on a two-body approximation to the effective Hamiltonian, so it is difficult to make direct comparisons. However, we showed that for $q \leqslant 0.154$ the mapping of the binary Asakura–Oosawa model onto the effective one-component Hamiltonian based on pairwise additive Asakura–Oosawa potentials is exact and thus we *can* compare the phase diagrams for $q = 0.1$. For this size ratio we find that the metastable fluid–fluid transition is shifted to unphysically high colloid packing fractions in the free-volume approach and that the fluid–solid transition is described slightly less well than in perturbation theory. Moreover, the free-volume theory does not yield the solid–solid transition, although it does give a spinodal instability in the solid phase. In order to assess the validity of the free-volume results at high q, direct simulations of the binary Asakura–Oosawa model should be performed. However, this will require new simulation techniques. This issue will be addressed in future work. Finally

we made comparisons between the phase diagrams calculated for the Asakura–Oosawa pair potential and those from the equivalent depletion potential treatment of the additive binary hard-sphere mixture. For $q = 0.1$ the fluid–solid and solid–solid phase boundaries are very similar in both models, reflecting the similarity between the two effective potentials at low values of η_2^r. At higher values of q the interesting features of the phase behaviour occur at large values of η_2^r where the two effective potentials are very different, and this leads to the absence of a fluid–fluid transition for the additive binary hard-sphere case.

We turn now to the possible relevance of our results for real mixtures. In experiments on sterically stabilized polymethylmethacrylate (PMMA) particles and non-adsorbing polystyrene in decalin, similar trends of the phase diagrams as functions of q were found to those of the present simulations [6]. However, the three-phase coexistence disappears, i.e. the liquid phase becomes 'marginal', at a size ratio of $q \leqslant 0.25$ in these experiments [6]. A possible reason for the discrepancy in the crossover value of q might be the neglect of three-body and higher-body terms in the simulations and in the perturbation theory. Note, however, that the free-volume approach, which incorporates some many-body effects, predicts a crossover value of $q \sim 0.32$, while direct simulations of a lattice model version of the Asakura–Oosawa model, which restricts the polymer spheres to a cubic lattice, estimate the crossover at $q \sim 0.45$ [10]. Another possible reason for the discrepancy with experiments is the non-ideality or deformability of the polymers. Direct simulations of colloids and ideal lattice polymers, which incorporate the flexibility of the polymer coils, estimate the crossover at $q \leqslant 0.43$, which is only slightly lower than the value cited above for the Asakura–Oosawa model with polymer spheres restricted to a cubic lattice [10]. Recently, depletion potentials have been calculated which include effects of the anisotropy of ideal polymer chains [27]. These provide a better account of the experimentally measured depletion potentials [27]. The polydispersity of the colloids and polymers might also be relevant, and the effect of polydispersity on the depletion forces was investigated in references [28] and [29]. How such modifications of the depletion potentials might affect phase behaviour remains a subject for investigation.

The colloid–colloid radial distribution function $g(r)$ and the structure factor $S(k)$ were calculated for the fluid phase, but close to the phase boundaries, for the pairwise-additive approximation to the effective Hamiltonian using both simulation and the PY integral equation theory. We found very good agreement between the PY results and those of simulations. Static colloid–colloid structure factors were measured recently for three colloidal liquids at their triple points. The system was PMMA and polystyrene in decalin and the three size ratios were $q = 0.57$, 0.37, and 0.24 [7]. As the liquid becomes more marginal (lower q), the height of the main peak of $S(k)$ changes very little, i.e. $S(k_m) \sim 2.5 \pm 0.2$. This result is surprising when we recognize that the colloid packing fraction for the liquid phase at the triple point decreases significantly upon decreasing q; $\eta_c = 0.333$ for $q = 0.24$, which is the marginal case. We might expect a lower value of $S(k_m)$ for a liquid with this value of η_c. In addition, a substantial increase of $S(k)$ at low k was found upon decreasing q. In figure 13, we plot $S(k)$ obtained from simulations for the liquid phase near the triple point (state-points B) for three values of q. Note that for $q = 0.4$ the liquid phase is not at the triple point. We find that $S(k_m)$, the height of the first peak of $S(k)$, is slightly larger for $q = 0.6$ than for $q = 0.8$, which is a little surprising given that η_c is 6 or 7% higher for the latter. However, this feature is not found in the PY results—see figures 2, 4, and 6. For $q = 0.4$ we find that $S(k_m)$ is reduced by about 0.4, or so, below the peak height for $q = 0.8$ and that $S(0)$ is increased above the values for $q = 0.6$ and 0.8. Such observations are consistent with the reduction in colloid packing fraction; $\eta_c = 0.42$ for state-point B at $q = 0.4$. Thus, the trends that we find in the simulation study are not as pronounced as those found in the experiments [7]. In particular, it is difficult to see how a pair potential of the Asakura–Oosawa type could yield $S(k_m) \sim 2.25$

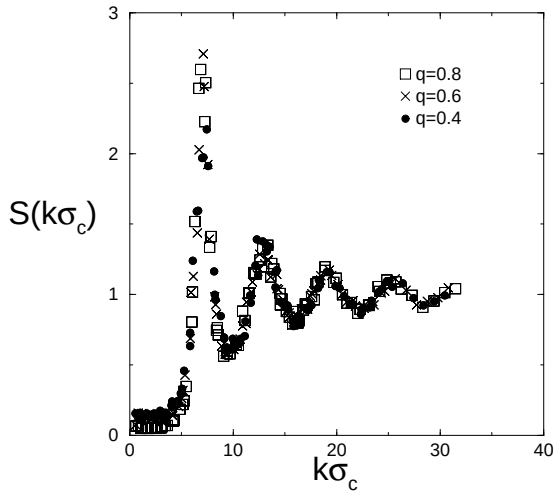

Figure 13. The structure factor $S(k\sigma_c)$ for the effective one-component system, based on the Asakura–Oosawa pair potential (8), with size ratios $q = 0.8$, 0.6, and 0.4. Each result refers to the liquid phase near the triple point (state-points B given in table 1 and in figure 1).

for $\eta_c = 0.333$. Whether the full binary Asakura–Oosawa model would produce significantly different colloid–colloid structure factors from those given here remains to be seen and this topic will be addressed in future work.

Acknowledgments

This work was made possible by financial support from the EPSRC under grant GR/L89013 and from the EPSRC Liquid Matter Network. We thank René van Roij, Jean-Pierre Hansen, and Ard Louis for stimulating discussions and Henk Lekkerkerker for some valuable comments.

References

[1] Asakura S and Oosawa F 1954 *J. Chem. Phys.* **22** 1255
Asakura S and Oosawa F 1958 *J. Polym. Sci.* **33** 183
[2] Vrij A 1976 *Pure Appl. Chem.* **48** 471
[3] Gast A P, Hall C K and Russel W B 1983 *J. Colloid Interface Sci.* **96** 251
[4] Lekkerkerker H N W, Poon W C K, Pusey P N, Stroobants A and Warren P B 1992 *Europhys. Lett.* **20** 559
[5] Leal Calderon F, Bibette J and Biais J 1993 *Europhys. Lett.* **23** 653
[6] Ilett S M, Orrock A, Poon W C K and Pusey P N 1995 *Phys. Rev.* E **51** 1344
[7] Moussaïd A, Poon W C K, Pusey P N and Soliva M F 1999 *Phys. Rev. Lett.* **82** 225
[8] Ye X, Narayanan T, Tong P, Huang J S, Lin M Y, Carvalho B L and Fetters L J 1996 *Phys. Rev.* E **54** 6500
[9] Louis A A, Finken R and Hansen J-P 1999 *Europhys. Lett.* **46** 741
[10] Meijer E J and Frenkel D 1994 *J. Chem. Phys.* **100** 6873
[11] Dijkstra M, van Roij R and Evans R 1998 *Phys. Rev. Lett.* **81** 2268
Dijkstra M, van Roij R and Evans R 1999 *Phys. Rev. Lett.* **82** 117
Dijkstra M, van Roij R and Evans R 1999 *Phys. Rev.* E **59** 5744
[12] Hansen J-P and McDonald I R 1986 *Theory of Simple Liquids* (London: Academic)
[13] Hansen J-P and Verlet L 1969 *Phys. Rev.* **184** 151
[14] Hagen M H J and Frenkel D 1994 *J. Chem. Phys.* **101** 4093
[15] Bolhuis P and Frenkel D 1994 *Phys. Rev. Lett.* **72** 2211
Bolhuis P, Hagen M and Frenkel D 1994 *Phys. Rev.* E **50** 4880

[16] Carnahan N F and Starling K E 1969 *J. Chem. Phys.* **51** 635
[17] Hall K R 1972 *J. Chem. Phys.* **57** 2252
[18] Hoover W G and Ree F H 1968 *J. Chem. Phys.* **49** 3609
[19] Press W H, Flannery B P, Teukolsky S A and Vetterling W T 1992 *Numerical Recipes in Fortran* (New York: Cambridge University Press)
[20] See, e.g., Magli R, Barocchi F, Chieux P and Fontana R 1996 *Phys. Rev. Lett.* **77** 846
[21] Vliegenthart G A, Lodge J F M and Lekkerkerker H N W 1999 *Physica* A **263** 378
[22] Barker J A and Henderson D J 1967 *J. Chem. Phys.* **47** 2856
[23] Verlet L and Weis J J 1972 *Phys. Rev.* A **5** 939
[24] Kincaid J M and Weis J J 1977 *Mol. Phys.* **34** 931
[25] Götzelmann B, Evans R and Dietrich S 1998 *Phys. Rev.* E **57** 6785
[26] Götzelmann B, Roth R, Dietrich S, Dijkstra M and Evans R 1999 *Europhys. Lett.* **47** 398
[27] Triantafillou M and Kamien R D 1999 *Phys. Rev.* E **59** 5621
[28] Walz J Y 1996 *J. Colloid Interface Sci.* **178** 505
[29] Chu X L, Nikolov A D and Wasan D T 1996 *Langmuir* **12** 5004